International Journal of Greenhouse Gas Control 74 (2018) 155–173

Contents lists available at ScienceDirect

International Journal of Greenhouse Gas Control

journal homepage: www.elsevier.com/locate/ijggc

A comprehensive modeling of the hybrid temperature electric swing adsorption process for CO_2 capture

S. Lillia[a], D. Bonalumi[a,*], C. Grande[b], G. Manzolini[a]

[a] Department of Energy Politecnico di Milano, Via Lamruschini 4, 20156, Milano, Italy
[b] SINTEF Materials and Chemistry. P.O. Box 124 Blindern, N0314, Oslo, Norway

ARTICLE INFO

Keywords:
Temperature Electric Swing Adsorption
Carbon capture
CO_2 capture
NGCC
EGR
Zeolite Molecular Sieve 13X (MS13X)

ABSTRACT

Adsorption technologies provide high selectivity and low energy consumption making this technique very attractive to be employed in post-combustion carbon capture. In this publication, a material made of activated carbon and zeolite 13X is considered for a hybrid process termed Temperature Electric Swing Adsorption (T/ESA). This hybrid T/ESA can work as a traditional Temperature Swing Adsorption (TSA) heated by hot gas, but can also increase the temperature of the adsorbent very fast by Joule effect as long as the activated carbon provides a continuous conductive matrix for electricity. This paper discusses a detailed modeling of the T/ESA process when applied to three cases. The first case is the simulation of the T/ESA process with exhaust with 12% of CO_2 concentration, which has been chosen to validate the model against literature results. The second and third case studies consider the T/ESA application in a natural gas combined cycle (NGCC) traditional power plant, and in a NGCC plant with exhaust gas recycle (EGR). These cases were selected to investigate the adsorption technology at low CO_2 concentration and quantify the benefit of the EGR for carbon capture applications. Starting from an NGCC overall electric efficiency of 58.3% LHV based, the efficiency of the NGCC with T/ESA technology reduces to 35.3% while with EGR is 38.9% against the 49.9% with the MEA absorption plant. The same results are confirmed by the SPECCA index 13.05 MJ_{LHV}/kg_{CO2} to 9.64 MJ_{LHV}/kg_{CO2} against the reference of 3.36 MJ_{LHV}/kg_{CO2}. The energy penalty of the T/ESA is significant because of electric consumptions required for the heating and fast cooling of the adsorbent.

1. Introduction

Power generation is one of the major stationary sources of CO_2 emissions. Existing and future power plants will rely on fossil fuels with consequent CO_2 emissions if no corrective action is taken. One possibility is to remove the carbon dioxide out of the exhaust gases preventing emissions to atmosphere. Currently, CO_2 removal technologies are still under industrial testing (Banks and Bibland-Pritchard, 2015). Research activities are developing innovating CO_2 removal techniques to reduce the energy and economic penalties. The flue gas of current power plants both natural gas and coal based is a mixture of nitrogen, oxygen, carbon dioxide and water, plus other contaminants in limited concentration. One major advantage of the post-combustion capture layout is that it can be used for new power plants but also for retrofitting to the existing ones (Vitillo et al., 2017).

The most studied post-combustion technology is chemical absorption. In particular, Mono Ethanol Amine (MEA) represents the reference chemical for this purpose (Giuffrida et al., 2013; Wang et al., 2011; Sanchez Fernandez et al., 2014). Other substances have been proposed to decrease the energy penalty of carbon capture on the net power produced by the power plant. Piperazine (Sanchez Fernandez et al., 2014; Kvamsdal et al., 2014) and ammonia (Bonalumi and Giuffrida, 2016; Bonalumi et al., 2016) are examples of alternative solvents, but still with relevant energy penalty. Nevertheless, the third generation solvents are not far from the theoretical CO_2 separation minimum (Kim and Lee, 2017).

Other technologies that are studied encompass membranes (Gazzani et al., 2014) and processes using sorbents (Li et al., 2016; Jansen et al., 2015). They are mainly studied for coal-fired flue gases where the content of CO_2 is around 10–15%, since their efficiency is strictly connected to the partial pressure of CO_2. When the flue gas comes from a natural gas fired power plant, the content of CO_2 is between 3 and 5% so higher selectivity is required to separate CO_2 with purity above 95%. Adsorbents provide a large surface area that can be used for this purpose. Among different sorbents, Zeolite 13X was proposed for CO_2 capture in a Pressure Swing Adsorption (PSA) process. Thakur et al. (Thakur et al., 2015) developed a PSA cycle for a gas with molar composition of 20% CO_2/80% N_2. (Song et al., 2015) discussed an

* Corresponding author.
E-mail address: davide.bonalumi@polimi.it (D. Bonalumi).

https://doi.org/10.1016/j.ijggc.2018.04.012
Received 20 October 2017; Received in revised form 3 April 2018; Accepted 12 April 2018
Available online 08 May 2018

Nomenclature

Acronyms

CCR	Carbon capture ratio
CSS	Cycle steady state
EGR	Exhaust gas recycle
ESA	Electric swing adsorption
GT	Gas turbine
HD	Specific heat duty
HRSG	Heat recovery steam generator
HTF	Heat transfer fluid
MEA	Mono ethanol ammine
MOF	Metallic organic framework
NGCC	Natural gas combined cycle
PCHE	Printed circuit heat exchanger
PSA	Pressure swing adsorption
ST	Steam turbine
TSA	Temperature swing adsorption
T/ESA	Hybrid temperature electric swing adsorption

Symbols

α_{HC}	Surface of the honeycomb channel [m^2]
E_{bed}	Internal energy of the adsorption bed [J]
HD_i	Specific heat duty of the i source [J/kg]
I	Electric current [A]
$IP_{N,i}$	Parameter N of the i specie in the aspen isotherm equation
K_i	Constant of the i specie in the extended langmuir isotherm equation [1/bar]
K_i^0	Constant of the i specie in the extended langmuir isotherm equation [1/bar]
m_i	Mass of the i component [kg]
$\dot{n}_{i,j}$	Mole flow of the i specie in j stream [mol/s]
P_i	Partial pressure of the i specie [Pa]
q_i	Solid loading of the i specie [mol/kg_{ads}]
$q_{i,max}$	Asymptotic solid loading of the i specie [mol/kg_{ads}]
Q_i	Heat duty of the i source [J]
$\dot{Q}_{HEAT}$	Heat supplied to the adsorption column [J]
R_i	Electric resistance of the of the i component [Ω]
R_g	Universal gas constant [J/(K mol)]
t_i	Time of the i cycle step [s]
T_i	Temperature of the i component [K]
v_{HC}	Average velocity of the gas in the honeycomb [m/s]
W_i	Electric energy from the i source [J]
w_i	Specific electric energy from the i source [J/kg]

Greek symbols

ΔH_i	Heat of adsorption of the i specie [J/mol]
ϕ	Purity of CO_2 captured [Pa s]
μ_i	Viscosity of the i specie [Pa s]
Π_{ads}	Productivity of the adsorption material [kg_{CO2}/(t h)]

alternative PSA process that reduces the energy impact of the capture plant by exploiting part of the exothermic heat of adsorption for the regeneration.

When the flue gas has a low CO_2 content, Temperature Swing Adsorption (TSA) process can be adopted as proposed by (Mérel et al., 2006). The main drawback of TSA process is the long time required for desorption cycles, that can be reduced by maximizing the contact area between the hot gas and the adsorbent (Bonnissel et al., 2001). One possible process that can speed up the heating of the adsorbent is Electric Swing Adsorption (ESA), where a low voltage electric current is employed to heat the adsorbent by Joule effect (Petkovska et al., 1991; Burchell et al., 1997; Yu et al., 2007; Sullivan et al., 2004). A review of ESA application for gas separation and purification is available (Ribeiro et al., 2014). One disadvantage of the ESA process is that the temperature increase is achieved by using electric power; electric power has a higher exergetic value than heat used in TSA process. (Grande and Rodrigues, 2008) proposed an ESA application for CO_2 capture with activated carbon honeycomb monolith.

Among the several adsorbents that are suggested in literature (Kenarsari et al., 2013), the most studied ones are zeolites (Yaumi et al., 2017; Girimonte et al., 2017; Masala et al., 2017). They are thermally stable crystalline materials with pores of 0.3–1.3 nm diameter. They can be applied for CO_2 capture in adsorption processes and also within membranes (Gkanas et al., 2015). However, since they do not conduct electricity, they have to be embedded in a conductive matrix to promote heating by Joule effect. In this case, the matrix that provides electrical conductivity to the adsorbent is activated carbon.

The main objective of this work is to evaluate a hybrid Temperature Electric Swing Adsorption (T/ESA) cycle as an innovative second-generation technique to capture CO_2 from flue gases. The ESA process is mentioned in several reports as one possible technique to capture CO_2 from flue gases, but so far, this process was only commercially employed to remove volatile organic compounds (Subrenat and Le Cloirec, 2006).

In this work, particular interest will be given to the modeling of the T/ESA process applied to NGCC. The modeling was carried out using Aspen Adsorption (Aspentech, 2003). The T/ESA process is applied to a well-established reference NGCC power plant defined in the European benchmark taskforce (EBTF) document (Sanchez Fernandez et al., 2014). Differently from other technologies like absorption or membranes, the T/ESA process is unsteady and cyclic so sequential different steps are necessary to regenerate the adsorbent in an efficient way. The cyclic configuration is able to achieve a high purity CO_2 stream is based on a previous work (Grande and Rodrigues, 2008). The main innovation of this work is to model a dual hybrid process, with two different sources to provide heat for the regeneration steps: using fast heating by electric power, steam taken from the power plant and heat recovery steps during the cyclic process of adsorption. The following sections will present the T/ESA process and the modeling description. Then, T/ESA integration in the considered power cycle will be discussed and finally the results of the modeling activity will be presented.

2. T/ESA process description

This section discusses the T/ESA modeling approach adopted in this work to assess the performance when applied to fossil fuel power stations.

The first step for the capture plant process is the choice of the sorbent material. The materials considered for the T/ESA application must satisfy both the properties of high loading/selectivity to the CO_2 and the electric conductivity properties for the electric heating process. Regarding CO_2 capacity, promising materials considered for this application are zeolites (Cavenati et al., 2004; Ribeiro et al., 2013) and metallic organic frameworks (MOF's) (Xiang et al., 2012; Masala et al., 2016). For the T/ESA application, an interesting material is a honeycomb material obtained by co-extrusion of activated carbon and zeolite Molecular Sieve 13X (MS13X). This material can keep high capacity and selectivity at low partial pressures of CO_2 while the carbon provides the electrical conductivity.

An eight-step cycle is adopted after preliminary evaluations derived by the previous study on similar adsorption processes proposed in literature (Grande and Rodrigues, 2008; Grande et al., 2009; Joss et al.,

2017). This configuration was found to be the one that guarantees the lowest consumption while complying to the CO_2 purity and CO_2 capture sets as target.

The eight T/ESA cycle steps are reported in Fig. 1 and consist of:

1) Adsorption step, where the flue gases pass though the adsorption column and the CO_2 is selectively adsorbed by the material.
2) Recuperative pre-heating step, where the column is heated up by the heat recovered during the cooling stage. In this step, the adsorbent reaches a temperature close to the average temperature between the beginning and the end of the heating process. The CO_2 is desorbed, the pressure inside the column increases, and a highly concentrated CO_2 stream is sent to compression and storage.
3) Steam heating step, where the heating process continue using steam extracted from the steam turbine. This process heats the column to an intermediate temperature chosen between the end of recuperative pre-heating step and the maximum temperature of the cycle.
4) Electric heating step, where the column is heated up quickly to the maximum temperature by the Joule effect generated by applying a low voltage electricity to the adsorbent honeycomb.
5) Purge to capture step, where part of the nitrogen purified in the adsorption stage is recycled to the column to reduce the partial pressure of the carbon dioxide in the column and desorb it from the solid phase. In this step, the gas that leaves the column has still a high purity of CO_2, hence it is sent to capture and storage.
6) Purge to recycle step, where the nitrogen rinse continues, but the outlet gas has a low concentration of CO_2. Hence, to avoid losing this CO_2 and increase the carbon capture ratio, the gas is recycled to the adsorption step.
7) Thermal recovery step, where the column is cooled down and the heat is recovered in the recuperative pre-heating step.
8) Cooling step, where the column is cooled down with water from the evaporative tower of the power plant to the initial temperature of the adsorption cycle.

The heating and cooling of the sorbent (step 2, 3, 7 and 8) is carried out using a heat transfer fluid (HTF) to preserve the CO_2 purity: the gas already inside the column is heated/cooled in a heat exchanger adding circulating fan consumptions.

The heat exchanger type selected for this application is the printed circuits heat exchanger (PCHE) (Dostal, 2004). The selection was based on the good performance of PCHE combined with its low production costs. In particular, in the second step, the gas is heated using the thermal recovery in the seventh step and water as HTF. In the third step, the steam from the steam turbine is used for further heating of the adsorbent. During the last cooling step, the water from the cooling tower of the power plant is used.

3. T/ESA model description

The T/ESA model, as previously described, is composed by several steps as well as auxiliary components. This paragraph provides the plant simulation processes and the scheduling design. The inputs for the overall simulation are the flue gas thermodynamic conditions (composition, pressure and temperature) and the mass flowrate after the water removal unit. These details are specified in the Aspen software where all the stages of the adsorption cycle are simulated. When the cycle simulation for a single column is performed, the last step is the scheduling design which considers the interaction of each column of the train. The process is iterated to reduce the power consumption or increase the productivity and avoid idle times. Fig. 2 sketches the overall methodology adopted for the simulation.

Therefore, the entire T/ESA process simulation required detailed modeling of the following aspects:

- Adsorption/desorption process and heat transfer in the adsorbent (ASPEN Dynamics);
- Heat transfer and design of the heat exchangers (excel macro)
- Auxiliary consumptions and power plant integration

The models for the different processes are described in detail below.

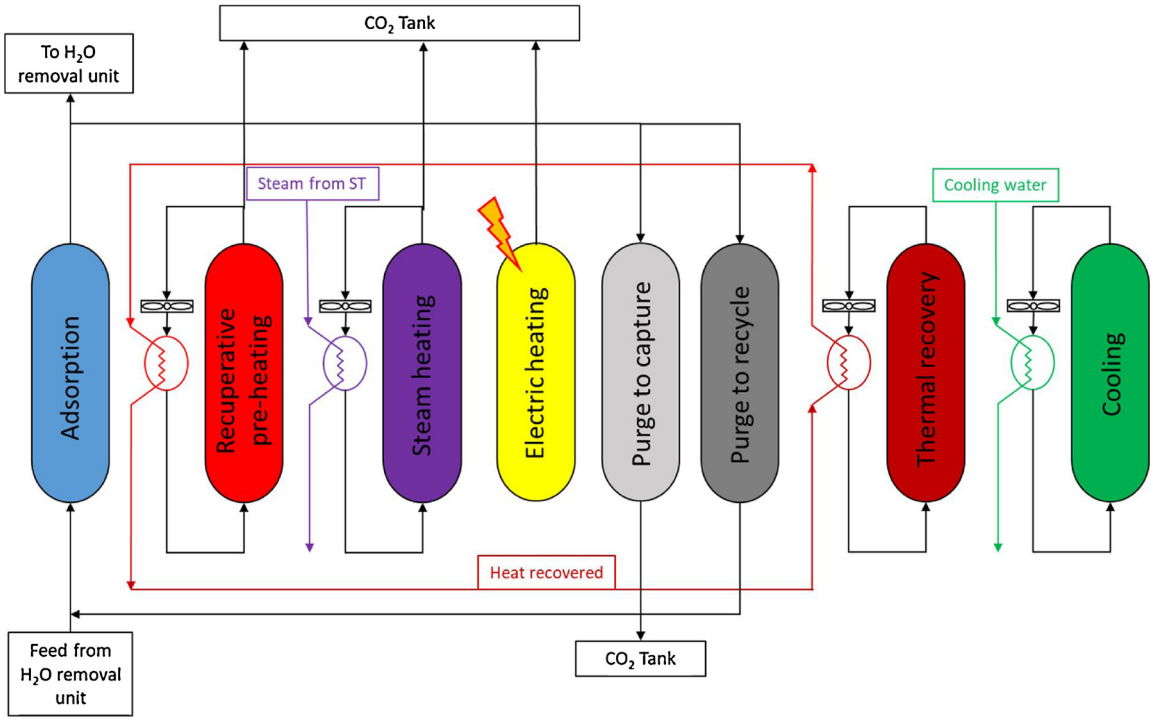

Fig. 1. T/ESA cycle steps and connections among the columns.

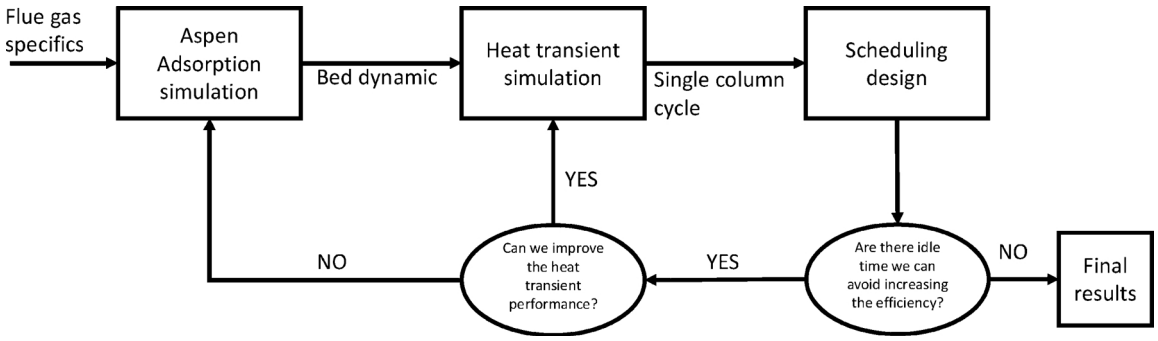

Fig. 2. Procedure of the overall simulation.

3.1. Adsorption/desorption process and sorbent characterization

The adsorption material selected for this application is the zeolite MS13X structured as a honeycomb composed by 80% MS13X zeolite and 20% activated carbon. The activated carbon matrix is needed to provide electrical conductivity to the honeycomb. Even when the activated carbon provides some adsorption capacity to the material, at low CO_2 concentration, the amount adsorbed is not high and what is observed is a reduction almost proportional to the amount of carbon present in the sample.

The experimental results are modelled with the Extended Langmuir isotherm equation which are available in Aspen Adsorption V8.4 environment. Extended Langmuir isotherm considers the competitive adsorption among the different species that compose the gas phase (nitrogen and carbon dioxide in this case). Eq. (1) reports the thermodynamic equations for the material isotherms where qi [mol/kg] is the solid loading of the specie i, qm,i [mol/kg] is the asymptotic loading of the specie i, Ki [1/bar] is the adsorption constant of the specie i and ΔHi [J/mol] is the heat of adsorption of the specie i. The fitting of the experimental data returns the parameters in Table 1 for the Eq. (1). The isotherms of both the expressions are presented in Fig. 3. Other physical properties and the pressure losses correlation are provided in Table 2.

$$q_i = \frac{q_{m,i} K_i P_i}{1 + \sum_i K_i P_i} \text{with} K_i = K_i^0 exp\left(\frac{-\Delta H_i}{R_g T}\right) \quad (1)$$

The pressure losses in the honeycomb were determined using a Darcy-type expression as shown in Table 2, where μgas is the viscosity of the gas phase, vhc the mean velocity of the gas inside the column and ahc the surface of each channel of the honeycomb.

Aspen Adsorption V8.4 allows the simulation of the entire process using one single column by defining the timing of each step. The column is initialized as filled with pure nitrogen, then the simulation runs until the convergence between two consecutive cycles is below a defined tolerance. This condition defines the regime of cyclic steady state (CSS) and the test tolerance on the relative difference is set at 10^{-3}. The simulation stops when the column reaches cyclic steady state. The results of all the profiles of the last cycle are taken as the results of the designed cycle and used to determine the performance of the adsorption plant.

The assumptions for the Aspen simulation are (Aspentech, 2003):

- Carbon capture ratio above 90%
- CO_2 purity above 95%
- Material balance, convection with estimated dispersion
- Momentum balance with Karman-Kozeny assumption
- Mass transfer from the bulk gas to the pores assumed with a linear mass transfer coefficient proportional to the partial pressure in the gas phase
- Energy balance non-isothermal with gas and solid conduction neglecting the heat losses with the environment
- One phase jacket heat exchanger in the adsorption column

The performance parameters which describes the adsorption cycle are: (i) Carbon capture ratio (CCR), (ii) the CO_2 purity, (iii) the specific Heat Duty (HD) and the productivity of the adsorption material (Πads).

The Carbon capture ratio (*CCR*), which is defined as the fraction of the CO_2, captured in a cycle on the total CO_2 at the inlet of the CO_2 capture process as in Eq. (2)

$$CCR = \frac{\int_{t_{st}}^{t_{end}} \dot{n}_{CO_2,capt}\, dt}{\int_{t_{st}}^{t_{end}} \dot{n}_{CO_2,in}\, dt} \quad (2)$$

where $\dot{n}_{CO_2,capt}$ [mol/s] is the molar flow of CO_2 to the CO_2 capture tank, $\dot{n}_{CO_2,in}$ [mol/s] is the molar flow of CO_2 in the flue gases from the water removal unit, tst [s] is the time at which the cycle starts and tend [s].

The CO_2 purity (ϕ), which is the molar fraction of the CO_2 in the flue gas sent to the CO_2 capture tank, is defined as in Eq. (3):

$$\phi = \frac{\int_{t_{st}}^{t_{end}} \dot{n}_{CO_2,capt}\, dt}{\int_{t_{st}}^{t_{end}} (\dot{n}_{CO_2,capt} + \dot{n}_{N_2,capt}) dt} \quad (3)$$

where $\dot{n}_{N_2,capt}$ [mol/s] is the molar flow of N_2 to the CO_2 capture tank.

The specific heat duty (*HD*) for the regeneration of the adsorbent which is the total heat provided to the adsorption bed on the total CO_2 captured

$$HD = \frac{\int_{t_{st}}^{t_{end}} \dot{Q}_{heat}\, dt}{\int_{t_{st}}^{t_{end}} \dot{n}_{CO_2,capt}\, dt} \quad (4)$$

where $\dot{Q}_{heat}$ [MW] is the thermal heat power provided to the adsorption column by the thermal recovery, the steam and the electricity during the steps 2, 3 and 4 described in the paragraph 2.

The productivity of the material Πads [$kg_{CO2}/(ton_{ads}\, h)$] can be defined as in Eq. (5)

$$\Pi_{ads} = \frac{\int_{t_{st}}^{t_{end}} \dot{m}_{CO_2,capt}\, dt}{t_{cycle} * m_{ads}} \quad (5)$$

where at the numerator there is the mass of CO_2 captured [kg/h] by a single column in a cycle and at the denominator the mass of adsorbent material in a column mads [ton] and the time of the cycle tcycle [h].

Table 1
Values for equation (1).

Isotherms parameters	CO_2	N_2
R_g [J/mol/K]	8.31	8.31
$q_{m,i}$ [mol/kg]	3.00	3.00
K_i^0 [1/bar]	4.25E-07	3.33E-05
$(-\Delta H_i)$ [J/mol]	4.50E+04	2.02E+04

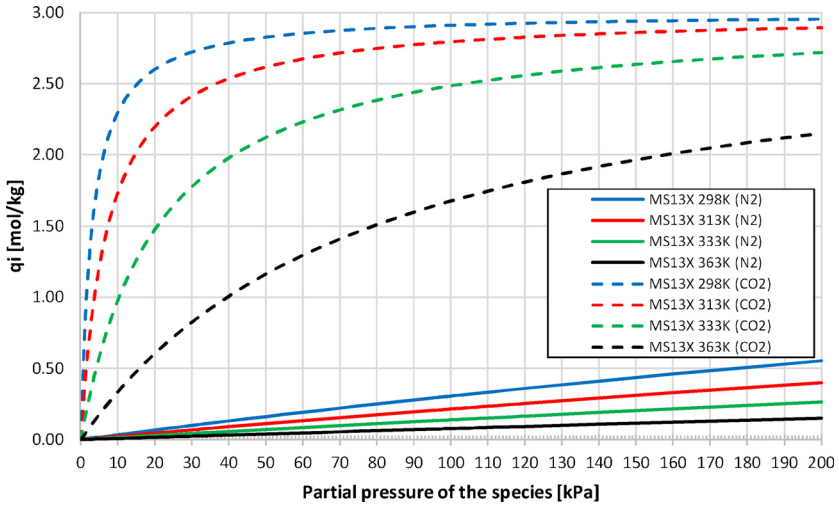

Fig. 3. Adsorption isotherms of hybrid material composed by zeolite 13X and activated carbon: N_2 solid lines, CO_2 dashed lines.

Table 2
Physical parameters of the zeolite-carbon hybrid honeycomb and pressure losses correlation of the zeolite honeycomb.

Parameter	Value
Adsorbent heat capacity [J/(mol*K)]	900
Wall density [kg/m^3]	1166.7
Wall porosity [−]	0.4
Pressure losses [Pa/m]	$\frac{-dP}{dz} = \frac{667.3482 * \mu_{gas} * v_{hc}}{2 * a_{hc}^2}$
Mass transfer coefficient of N_2 [1/s]	1
Mass transfer coefficient of CO_2 [1/s]	0.1

The simulation in Aspen is focused on the dynamic of the adsorption bed in every step of the cycle. The heat transients in Aspen are simulated as a thermal power inlet in the column since there is not a model of a PCHE heat exchanger which is the technology chosen in this layout.

3.2. Heat transfer model

The heat transient model is an Excel file with a macro where the heat exchanged in the PCHE between the thermal fluid and the gas inside the column is calculated according to models available in literature (Dostal, 2004). The gas is firstly blown by a fan in a closed circuit, then into the PCHE where it heats up exchanging heat with the HTF, and finally it passes though the bed where heat transfer between gas and honeycomb occurs. The power consumption of the fan balances the pressure drops of the honeycomb and the PCHE. This approach is used in the 2nd, the 3rd where the column is heated, the 7th and the 8th steps where the column is cooled. In the 2nd step, one side of the PCHE has water that recovers the heat of the 7th stage, on the other side the heated gas inside the column. Vice versa, the 7th step has water that recovers the heat from the column and supplies it to the 2nd step, indeed the stages 2nd and 7th are matched. One side of the 3rd step uses steam as HTF whilst column gas on the other side, the 8th step has water from the cooling tower to cool the column. For all these steps, the optimization parameters are: (i) the size of the PCHE, (ii) the channel dimensions of the honeycomb and (iii) the mass flow of the column gas circulated in the PCHE. The trade-off is between pressure losses, consequently the power consumption of the fan, and the heat exchanged and consequently the productivity of the adsorption cycle (i.e. the higher the gas flowrate the quicker is the heating/cooling step with advantages in terms of productivity, but with the drawbacks for the fan electric consumptions).

Finally, the 4th step, where the adsorption column is heated with electricity, is calculated simply as the energy balance between the electric heat provided by Joule effect to the bed. The equation describing the bed temperature increase is described in Eq. (6)

$$\frac{dE_{bed}}{dt} = m_{bed} c_{p,bed} \frac{dT_{bed}}{dt} = R_{bed} I^2 \tag{6}$$

where Ebed is the internal energy of the bed [J], mbed the mass of the bed [kg], cp,bed the specific heat of the bed [J/(kg K)], Tbed [K] the average bed temperature, Rbed [Ω] the electric resistance of the bed and the I [A] the current in the bed. In this step, the free parameter is the voltage applied to the honeycomb to heat up the bed as fast as possible to increase the productivity without exceeding the technologic limits of the electrodes (Ribeiro et al., 2012).

The heat transient simulation assesses the fan electric consumption, the heat recovered, the heat supplied by the steam and the heat supplied with the electricity. Main parameters defined on CO_2 captured base ($kg_{CO_2 captured}$) are reported in Eqs. (7)–(12):

$$w_{el,fans}(\text{specific fan electric duty}) = \frac{W_{el,fans}}{m_{CO_2\,capt}} \left[\frac{MJ}{kg_{CO_2}}\right] \tag{7}$$

$$HD_{steam}(\text{specific heat duty by steam bleeding}) = \frac{Q_{steam}}{m_{CO_2\,capt}} \left[\frac{MJ}{kg_{CO_2}}\right] \tag{8}$$

$$HD_{el}(\text{specific heat duty by electricity}) = \frac{Q_{el}}{m_{CO_2\,capt}} \left[\frac{MJ}{kg_{CO_2}}\right] \tag{9}$$

$$HD_{rec}(\text{specific heat recovered}) = \frac{Q_{rec}}{m_{CO_2\,capt}} \left[\frac{MJ}{kg_{CO_2}}\right] \tag{10}$$

$$w_{fans,rec}(\text{specific fan electric duty recovered}) = \frac{W_{fans,rec}}{m_{CO_2\,capt}} \left[\frac{MJ}{kg_{CO_2}}\right] \tag{11}$$

$$W_{el,\,loss\;ST}\ (\text{specific electric penalty due to the steam bleeding}) = \frac{W_{el,\,loss\;ST}}{m_{CO_2 capt}} \left[\frac{MJ}{kg_{CO_2}}\right] \tag{12}$$

where $W_{el,fans}[MJ]$ is the electric consumption for the fans during the heating and cooling step, $Q_{steam}[MJ]$ is the heat supplied by the steam condensation, $Q_{el}[MJ]$ is the heat supplied by electricity, $Q_{rec}[MJ]$ is the heat recovered by the column cooling, $W_{fans,rec}[MJ]$ is the heat due to the fan that is recovered during the recovery step, $E_{el,lossST}[MJ]$ is the

electricity loss for the steam bleeding from the steam turbine and $m_{CO_2 capt}[kg]$ the mass of the CO_2 captured in an adsorption cycle.

3.3. Integration with the power block, CO_2 compression and auxiliaries

This section describes the assumptions used to compute the electricity consumed by the power block/auxiliaries for capturing CO_2, namely (i) the power losses of the steam turbine due to the steam bleedings, (ii) the consumption of the CO_2 compressors and (iii) the fans needed to balance the water removal section and the T/ESA capture plant pressure drops (Fig. 4).

The effect of the steam extraction on the power generation is calculated starting from a typical expansion curve of a low-pressure turbine section. The curve is assumed to be a line connecting the inlet and outlet of the turbine on an entropy-enthalpy diagram (Fig. 5). The extraction pressure along the curve is determined by the regeneration temperature plus the temperature difference in the PCHE. Before entering the PCHE, the steam is attempered with part of the liquid water at the PCHE outlet. The extracted mass flow rate is defined by the energy balance in the reboiler for a given heat duty. The electric loss due to the steam extraction is computed as the power that would be generated by the extracted steam from the extraction state to the outlet state assuming that the expansion curve does not change (this assumption implies a custom turbine design including steam bleeding at the selected pressure and the same isentropic efficiency of the steam turbine without bleeding, which is reasonable as steam turbine are typically custom). The condensate is instead directed to the condenser. The integration of the exiting condensate with the heat recovery steam generator section (i.e. in the deaerator) is not considered in this work. The characteristic of the steam turbine are the same as the one adopted in the EBTF (Sanchez Fernandez et al., 2014).

The CO_2 compression section has been simulated with ASPEN according to the EBTF guidelines (Sanchez Fernandez et al., 2014). Compression work as well as amount of nitrogen remaining in the liquid CO_2 depends on RK-Soave thermodynamic model used in ASPEN ™ as well as binary coefficients adopted. Compression is divided into two parts: the first part, when the CO_2 is in vapor phase, consists of intercooled compressor composed by five stages with four intercoolers between each compression stage and one condenser. The second part, when CO_2 is liquid, includes a pump with a final aftercooler. The compressor provides an outlet pressure of 85 bar while the pump increases the pressure up to 110 bar, fixed as delivery pressure. All the water inside the CO_2 stream is removed before the fourth intercooler.

The isentropic efficiency of the compressor and the hydraulic efficiency of the pump are fixed and set equal to 0.85 and 0.75, respectively. The resulting overall consumption for CO_2 compression assuming 100% purity, which is the typical value for MEA separation process, is 310 kJ/kg_{CO2} (Sanchez Fernandez et al., 2014). The cycle used for this T/ESA process produces a less pure CO_2 and at a lower pressure, therefore the specific consumption will be 15 ÷ 16% higher.

Additional consumption, which should be taken into account, are related to fans. One fan is needed to overcome the pressure losses in the water removal and CO_2 separation sections; the exhaust gases at the outlet of the adsorbent must be kept at ambient pressure, therefore the fan is necessary to overcome the pressure losses in the capture section. This fan is placed upstream the entire section and is named Main fan (the same component is required in MEA plant).

4. T/ESA application to NGCC and NGCC with EGR

After its validation with other work on TSA process optimization availablein literature (reported in Appendix A), the model is applied to two different exhaust gases featuring compositions of a conventional natural gas combined cycle (NGCC) and a natural gas combined cycle with exhaust gas recycle (EGR). Finally, the performance of the different T/ESA cases will be compared to the amine scrubbing technology.

The EGR case is considered to evaluate the impact of the CO_2 concentration in T/ESA process; higher CO_2 concentration in the exhaust gases has benefits on the sorbent cyclic capacity, therefore reducing the

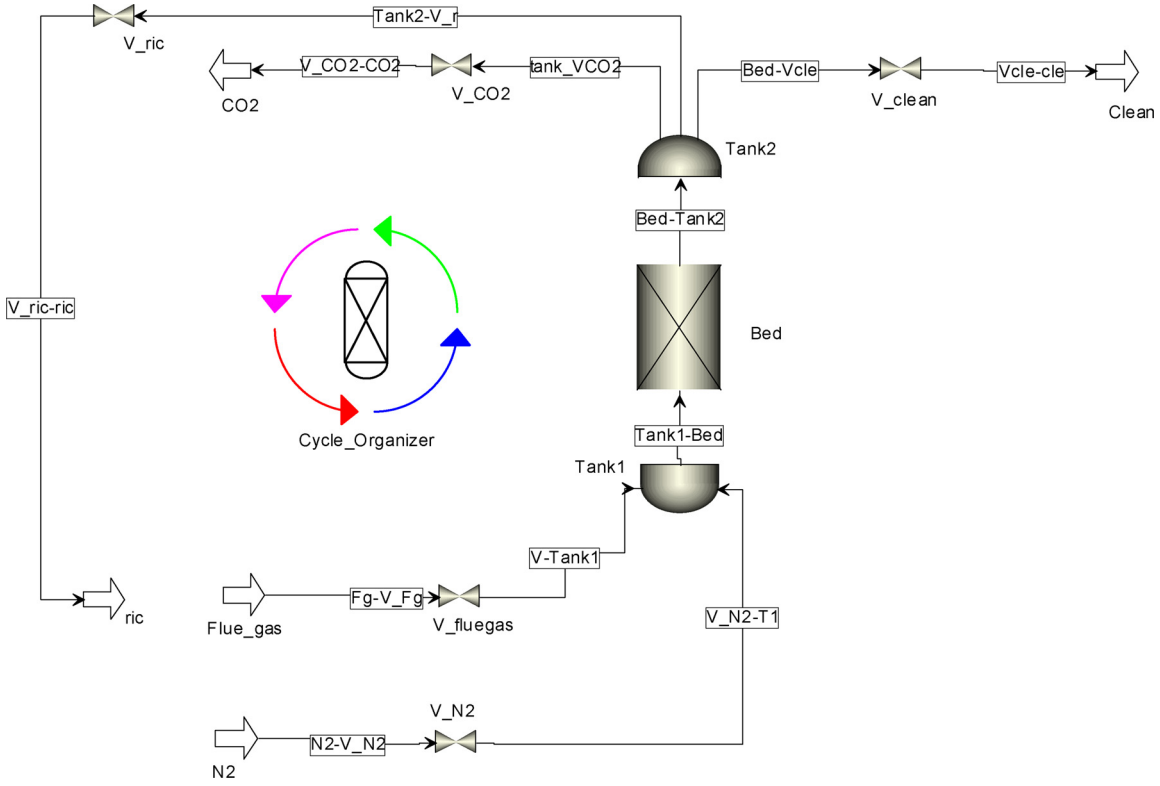

Fig. 4. Aspen Adsorption sketch of the column simulation.

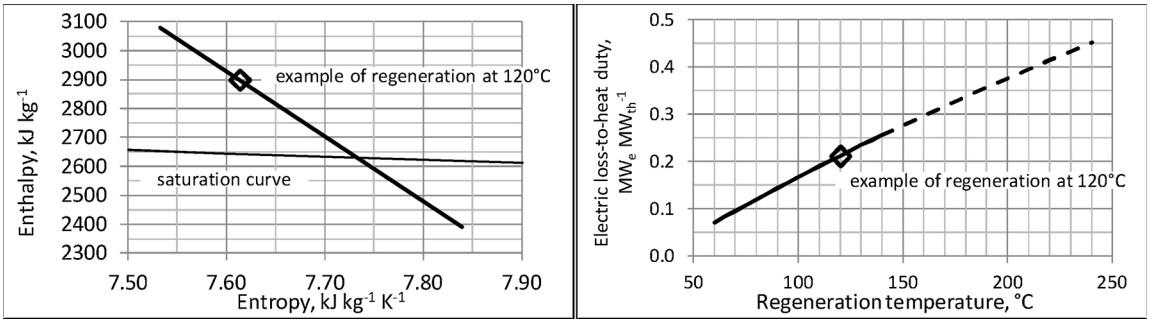

Fig. 5. Left: expansion curve in the enthalpy-entropy diagram of the low-pressure turbine from which the steam is extracted. Right: ratio of electrical loss-to-heat duty as a function of regeneration temperature (above 140 °C the curve is extrapolated because the computed pressure is higher than the inlet pressure). The diamond refers to a regeneration temperature of 120 °C.

regeneration energy required by the T/ESA cycle specific on the CO_2 captured.

In both cases, the overall process for CO_2 capture depicted in Fig. 6 is considered. Before the T/ESA process (the CO_2 removal Unit), exhaust gases are cooled and water separation section is necessary for drying the exhaust gases.

Zeolite 13X exhibits a significant affinity towards water. Therefore, it is required to remove water upstream the carbon dioxide unit to achieve acceptable carbon dioxide recovery rate and carbon dioxide purity. The pre-cooler is used to lower the flue gas temperature to 21 °C. By decreasing the gas temperature, most of the water is condensed and separated by gravity. The exhaust gas cooling is carried out into two steps: from 100 °C to 40 °C (same temperature assumed in MEA capture plants), a washing section which very limited consumptions is used, while the final cooling up to 21 °C is carried out with a chiller whose electric consumptions are taken into account. Activated alumina is used to adsorb the remaining water from the flue gas stream. Purified flue gases of the carbon dioxide removal unit are used to regenerate the activated alumina adsorbent reducing the energy penalties of the H_2O removal section only to fan power consumption needed to flow the gases against the pressures drops of the alumina adsorption bed. The temperature of the flue gases at the inlet of the carbon dioxide removal unit are at an average temperature of 30 °C.

The first power plant used for the preliminary assessment of T/ESA technology is based on two identical gas turbines (GT), each equipped with a heat recovery steam generator (HRSG) that share the same single steam turbine.

The net power output is 829.5 MW_{el} and the net electric efficiency is 58.3% LHV based (Sanchez Fernandez et al., 2014). Thermodynamic properties, composition and mass flowrate of two gas turbine exhaust gases are reported in Table 3, while the plant layout is reported in Fig. 7.

The second power plant considered is the NGCC with exhaust gas recycle (EGR). It has the same configuration as the plant previously described (two gas turbines with an HRSG with one steam turbine), but a fraction of the exhaust gases (35%) is cooled down and recirculated at the GT compressor inlet. The resulting net electric power output is 877 MW with a net electric efficiency of 58.3% LHV. The EGR has the aim to increase the CO_2 concentration in the exhaust. EGR changes the composition of the gas in the combustor of the gas turbine and consequently in the turbine. The net electric power increases because the effect of the higher CO_2 concentration increases the heat capacity and the mass flow rate of the flue gases elaborated by the GT and by the HRSG. The efficiency remains the same (58.3%) because double effect of the higher auxiliaries consumptions and the higher thermal input. The performance evaluation of the NGCC + EGR case was calculated with Thermoflex commercial software as in a previous work (Van der Spek et al., 2018). The vented composition is reported in Table 3 while the plant layout is shown in Fig. 8. Another positive aspect of EGR is the reduction of the flue gas flow to the CO_2 capture unit with values of about 40% (Sipöcz and Tobiesen, 2012; Lindqvist et al., 2014; Li et al., 2011; Evulet et al., 2009).

The overall CO_2 flowrate is 80.3 kg/s for the NGCC and 86.2 kg/s for the NGCC with EGR. When T/ESA capture section is considered with only electrical duty for the regeneration as in previous works (Grande et al., 2009), the operating condition of the power plant results unchanged. When the duty for the regeneration is both thermal and electric, the gas turbine operating condition will not change, while steam cycle power will reduce because of the steam bleeding. Simultaneously, power consumptions for heat rejection (which have limited impact) will reduce because the latent heat will be used for sorbent regeneration.

Finally, the index used to evaluate the efficiency of the considered carbon capture plant is the SPECCA (Specific primary energy for carbon

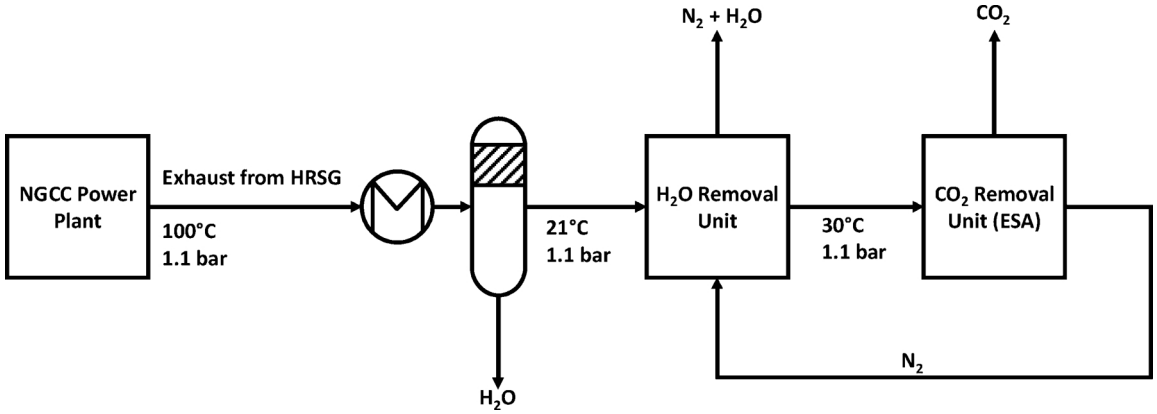

Fig. 6. Overall layout of a NGCC power plant with T/ESA as CO_2 capture technique.

Table 3
Specifications of the exhaust gas of the NGCC and NGCC with EGR power plant

Power Plant	Mass flow [kg/s]	Temperature [°C]	Pressure [Bar]	Composition, %mol Ar	N_2	O_2	CO_2	H_2O	NO_x
NGCC	1330.6	100	1.04	0.89	74.38	12.39	3.96	8.38	1.4E-03
NGCC + EGR	831.7	100	1.04	0.97	80.65	8.29	6.97	3.12	1.4E-03

capture) which is defined in Eq. (13)

$$SPECCA = \frac{\left(\frac{1}{\eta_{el,CCS}} - \frac{1}{\eta_{el,ref}}\right)}{(E_{CO_2,ref} - E_{CO_2,CCS})} * 3600 \left[\frac{MJ}{kg_{CO_2}}\right] \quad (13)$$

where ηel,CCS is the net electric efficiency of the plant with CCS, ηel,ref is the net electric efficiency of the reference plant without CCS, $E_{CO_2,CCS}$ are the CO_2 emissions [kg_{CO2}/MWh_{el}] of the plant with CCS and $E_{CO_2,ref}$ are the CO_2 emissions [kg_{CO2}/MWh_{el}] of the reference plant without CCS. This index shows the primary energy consumed for every kilogram of CO_2 captured in addition with respect to the reference power plant without the CO_2 capture plant.

5. Results and discussion

Results of the performance of the T/ESA cycle applied to the standard NGCC plant and the NGCC plant with EGR are here discussed. The validation case is reported in Appendix A. The results reflect the difference in the bed concentration and temperature profiles which affect the process performance due to the different CO_2 concentration in the exhaust gases. The geometric dimensions of the adsorption columns and the adsorbent honeycomb structure are in Table A.1 in the Appendix A. Finally, the results of the T/ESA plant integration with the power plant are presented and compared to a reference case with a MEA carbon capture plant applied to the NGCC power plant.

5.1. T/ESA applied to NGCC case

This section reports the results of the T/ESA process applied to the EBTF NGCC reference case (Sanchez Fernandez et al., 2014).

The composition of the flue gas treated after the water removal unit is 95.63% N_2 and 4.37% CO_2 and The cycle scheduling is designed with the simplified graphical approach explained by (Mehrotra et al., 2011) considering the constrain due to the time matching between a recuperative pre-heating phase and a thermal recovery phase and for this case is reported in Fig. 9.

The result is a train composed by 5 columns with a diameter of 6 m and a height of 2 m and a cycle of 2225 s. It can be noted the electric heating requires a very short time (around 1.5% of the cycle time), therefore supporting the principle of using electricity for the sorbent regeneration. However, the heating/cooling steps, which are mandatory, take 1370 s (61.5% of the overall cycle time) affecting the material productivity Π_{ads} which is34.57 [$kg_{CO2}/(t\ h)$].

The charts presenting the bed profiles are reported in Fig. 10. The first chart (i) in Fig. 10 shows the CO_2 bulk concentration at end of every cycle step. The gas phase inside the column rises together with the temperature during the heating step desorbing the CO_2. The second chart (ii) in Fig. 10 shows the solid loading. Since at the end of the adsorption step the solid is almost at the equilibrium with the CO_2 adsorption (except for the outlet part), it can be noted the impact of the temperature profile of the column (presented in the third chart (iii) in Fig. 10) on the CO_2 load of the solid: the temperature at the end of the adsorption step is lower at the beginning of the column (310 K) than in the central part where it is almost constant around 330 K. According to the temperature profile, the solid CO_2 loading is higher at the inlet of the column (almost by a factor of 2) than in the central part. Indeed, observing the isotherms of the material in Fig. 3, the effect of the temperature on the material loading is very high at low partial pressures. The fourth chart (iv) in Fig. 10 shows the CO_2 concentration in the gas phase in the column during the adsorption step. The adsorption step stops when the solid is saturated and a significant fraction of CO_2 is not adsorbed; indeed, at 445 s, the CO_2 concentration at the outlet is not close to zero like at the other times.

The heating and cooling transient steps are reported in Figs. 11 and 12. In Fig. 11, the three different heating steps recuperative preheating, steam and the electric heating are shown. The recuperative

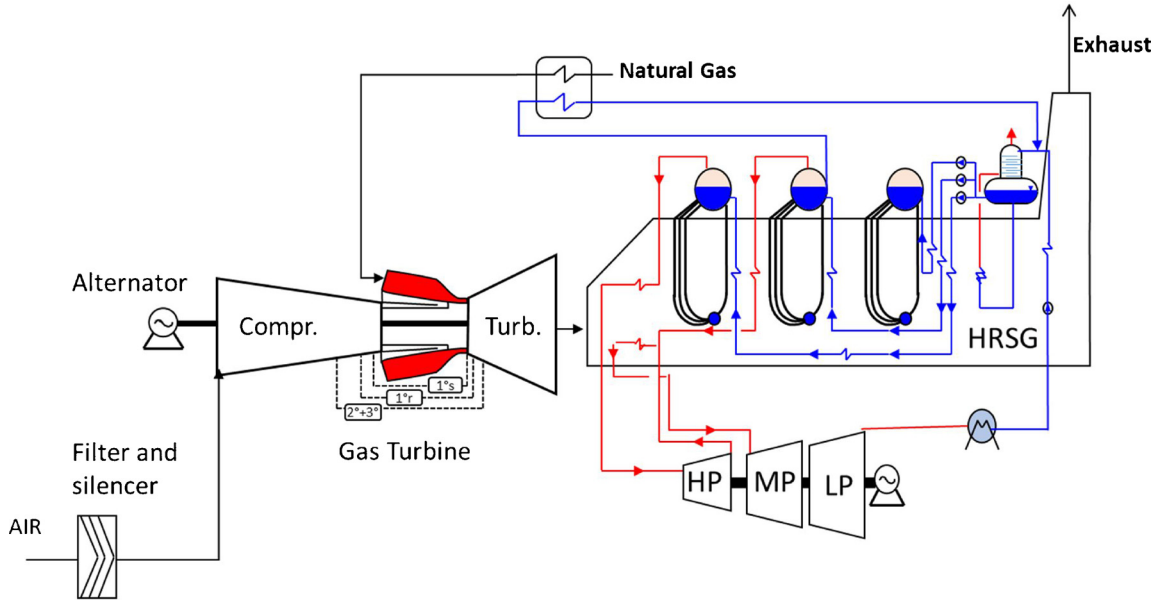

Fig. 7. Layout of the reference NGCC plant used in this study.

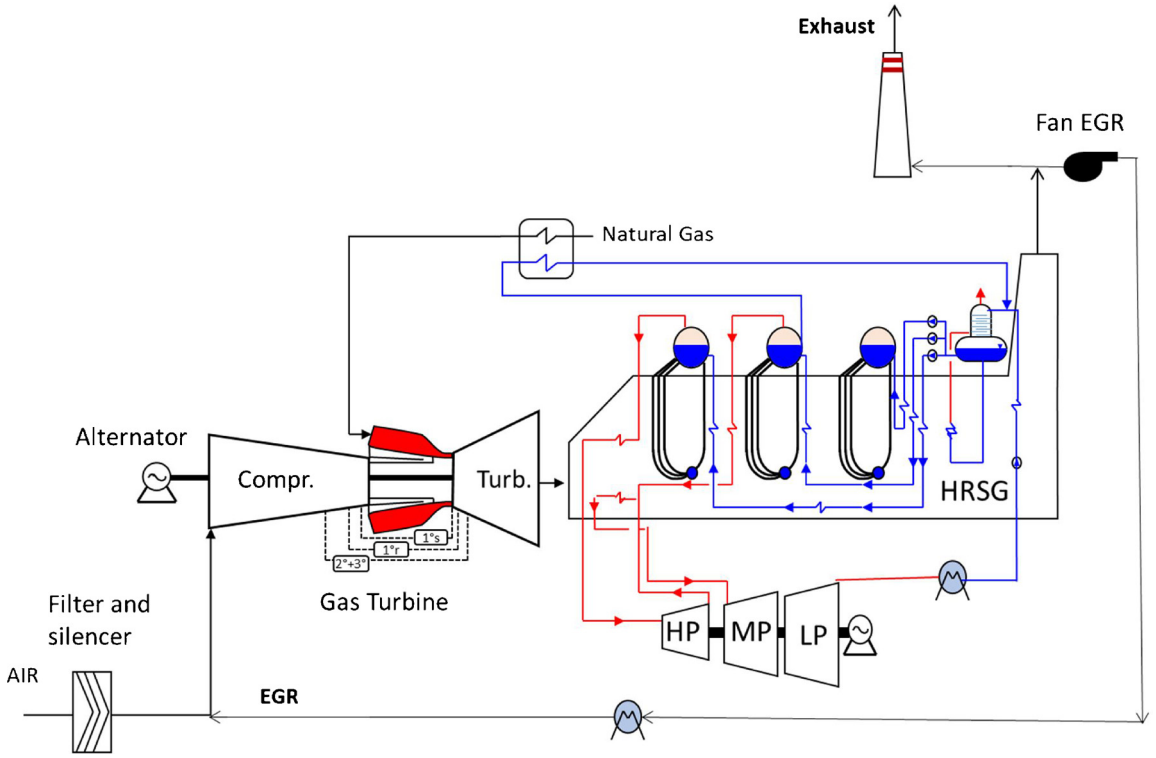

Fig. 8. Layout of the reference NGCC power plant with exhaust gas recycle (EGR).

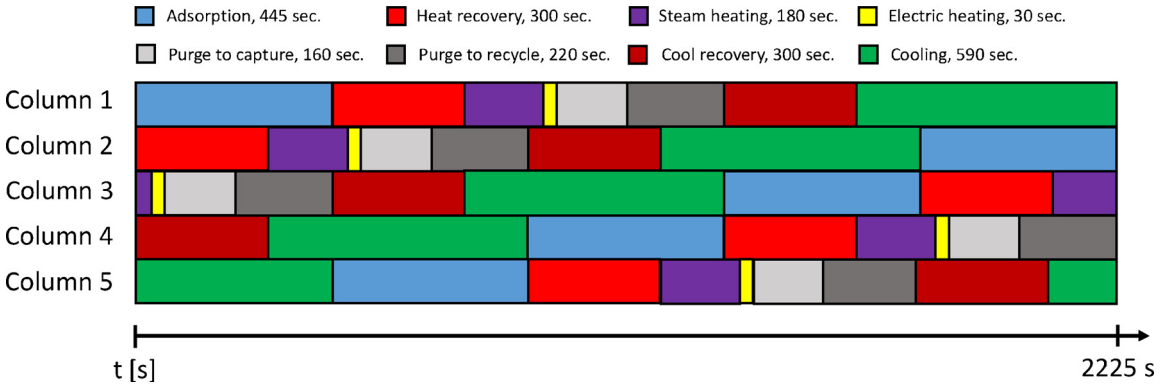

Fig. 9. Scheduling of the T/ESA cycle applied to the NGCC power plant.

pre-heating and the steam heating part are similar for what concerns the heat transfer and the difference of temperature between the fluid and the bed, while the electric heating is faster and represented by a strict line.

Fig. 12 shows the cooling recovery and the cooling steps. The cooling recovery step is coupled with the heating recovery step previously discussed, indeed, also the duration of the step coincides. The difference of temperature between the beginning and the end of the recuperative pre-heating step is higher than the difference of temperature between the beginning and the end of the cooling recovery step. This is due to the fans power needed for the gas circulation in the column that increase the difference of temperature in the heating step and reduce it in the cooling step. The cooling step, where the bed is cooled with cooling water, is the longest step.

Comparing the CO_2 solid load profiles at the end of the adsorption step and the electric heat step between the validation case presented in Appendix A (Fig. 13 (i)) and this case (Fig. 13 (ii)), the CO_2 solid load is higher in the former case consistently with the CO_2 concentration in the flue gas is higher (12% vs 4.37%) as expected with any sorbent. On the other hand, at the end of the electric heating the load profile is similar, consequently the sorbent cyclic capacity is higher resulting in a higher productivity. No significant difference in the heating and cooling steps can be noted for different CO_2 concentration.

The reduction of the CO_2 concentration in the flue gas has the effect to increase the adsorption time (and consequently the cycle time) and to reduce the loading of the adsorption bed together with the CO_2 captured in each cycle. These two effects penalize the productivity of the adsorption material (Π_{ads}equalto34.57 [kg_{CO2}/(t h)]) with respect to the productivity found in the validation case with a higher CO_2 concentration (Π_{ads} equal to 56.63 [kg_{CO2}/(t h)]).

Table 4 shows the performance of the T/ESA cycle (the meaning of each parameter is defined in paragraph 3.3).

Most of the heat supplied to the process is used for the material heating and the fan consumptions therefore it does not depend on the amount of CO_2 adsorbed but only to the heat transferred. The overall energy consumption does not vary significantly, but the captured CO_2 drops as consequence of the lower partial pressure in the gas phase resulting in the specific consumption increase.

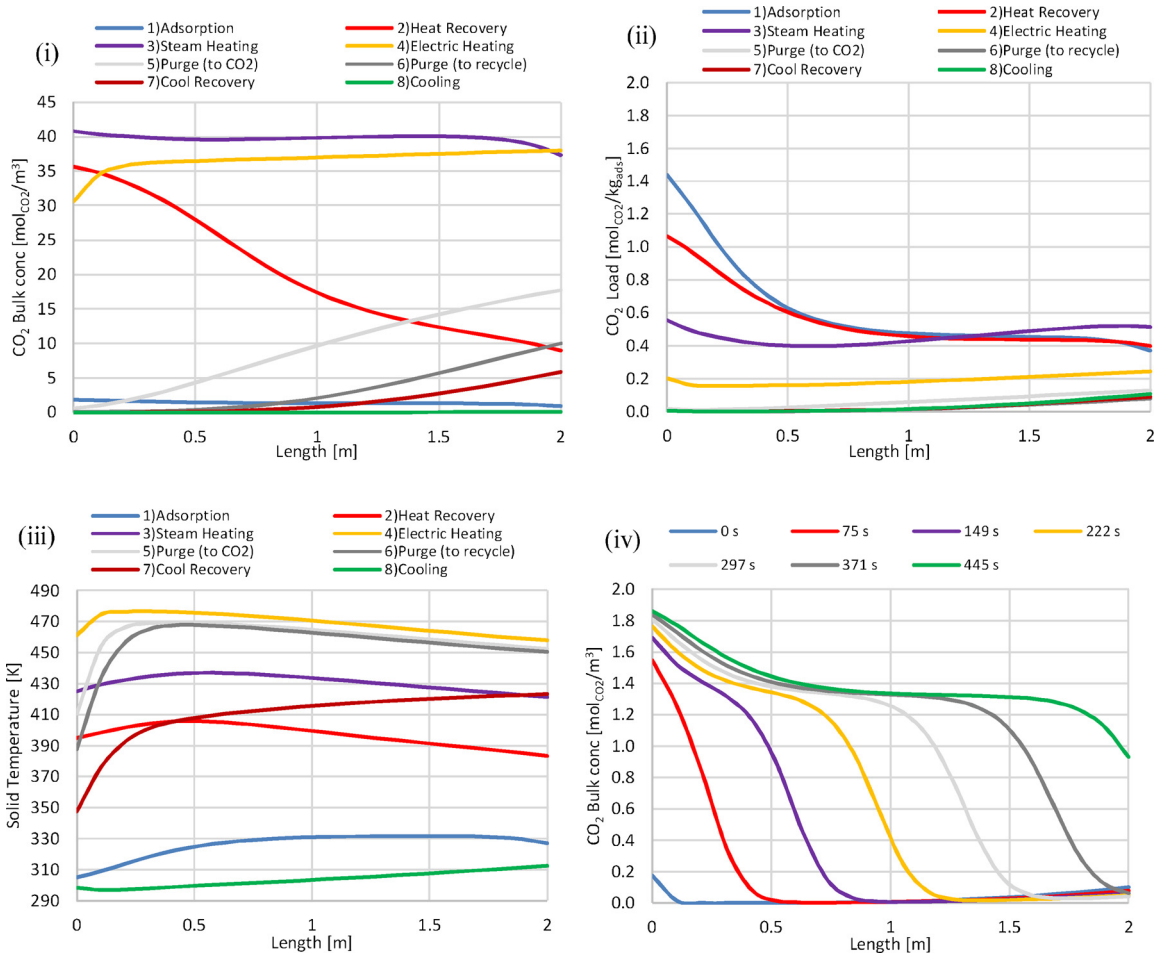

Fig. 10. The four charts present the results for the case with the NGCC flue gas of: (i) the bulk concentration profile of the CO_2 at the end of each step of the process, (ii) the CO_2 load profile at the end of each step of the process, (iii) the solid temperature profile at the end of each step of the process and (iv) the CO_2 bulk concentration in the column during the adsorption phase at different times.

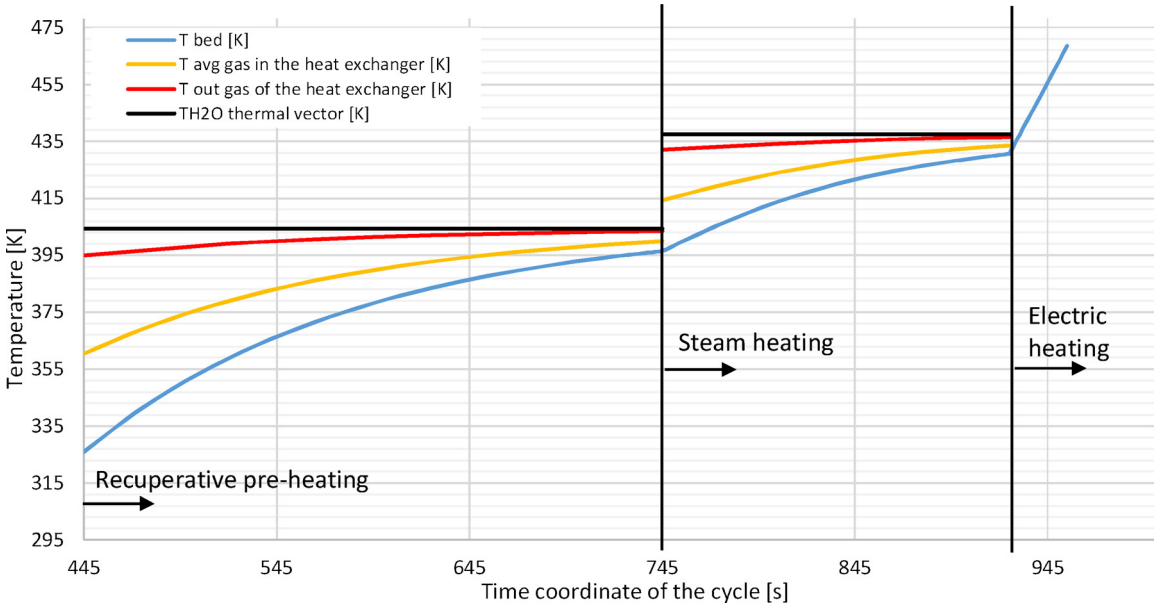

Fig. 11. Average temperature of the column during the heating steps of the T/ESA cycle applied to capture CO_2 from a NGCC power plant.

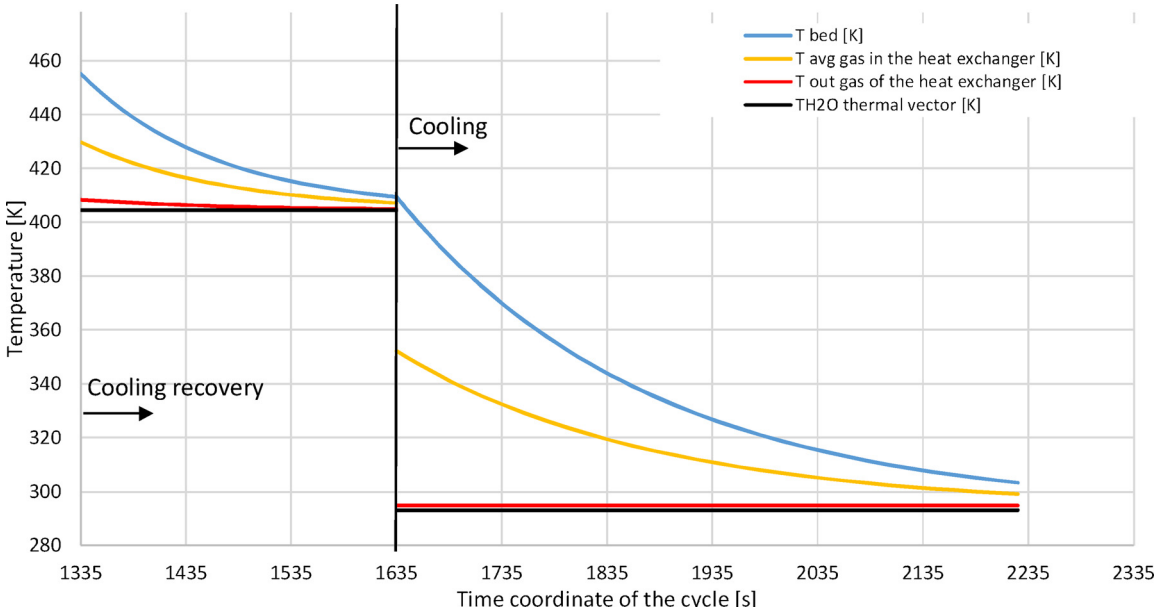

Fig. 12. Average temperature of the column during the cooling transient of the T/ESA cycle applied to capture CO_2 from a NGCC power plant.

5.2. T/ESA applied to NGCC with EGR plant

The results of the T/ESA process applied to reference case of the EBTF an NGCC plant (Sanchez Fernandez et al., 2014) with enhanced gas recycle (EGR) are here reported. The composition of the flue gas treated after the water removal unit is assumed equal to 92.74% N_2 and 7.26% CO_2. The cycle scheduling for this case is reported in Fig. 14.

The result is a train composed by 7 columns with a diameter of 6 m and a height of 2 m and a cycle of 1946seconds. Compared to the previous case, the adsorption step and the overall cycle time reduces by 40% and 15% respectively.

As in the case previously reported in paragraph 5.1, the charts representing the bed profiles are reported in Fig. 15 while the heating and cooling transient steps are reported in Figs. 16 and 17. The same considerations as in the previous case applies to this one.

The comparison of the CO_2 solid load profiles, especially at the end of the adsorption step and the electric heat step, is reported in Fig. 18(i) and (ii). At the end of the adsorption step, the CO_2 solid load of the first

Table 4
Performance of T/ESA process applied to NGCC power plant.

Parameter	Value
Molar flow of flue gas treated by each column train [kmol/s]	0.666
Carbon capture ratio (CCR) [%]	91.2
CO_2 purity [%]	94.7
Specific heat recovered (HD_{rec}) [MJ/$kg_{CO2capt}$]	3.121
Specific heat duty by steam bleeding (HD_{steam}) [MJ/$kg_{CO2capt}$]	1.291
Specific fan power recovered as heat duty ($w_{fans,rec}$) [MJ/$kg_{CO2capt}$]	0.545
Specific heat duty by electricity (HD_{el}) [MJ/$kg_{CO2capt}$]	2.131
Specific heat Duty ($HD = HD_{rec} + HD_{steam} + w_{fans,rec} + HD_{el}$) [MJ/$kg_{CO2capt}$]	7.089
Specific fan electric duty ($w_{el,fans}$) [MJ/$kg_{CO2capt}$]	1.218
Specific electric penalty due to the steam bleeding ($w_{el,loss\ ST}$) [MJ/$kg_{CO2capt}$]	0.397
Total specific electric penalty ($HD_{el} + w_{el,fans} + w_{el,loss\ ST}$) [MJ/$kg_{CO2capt}$]	3.968

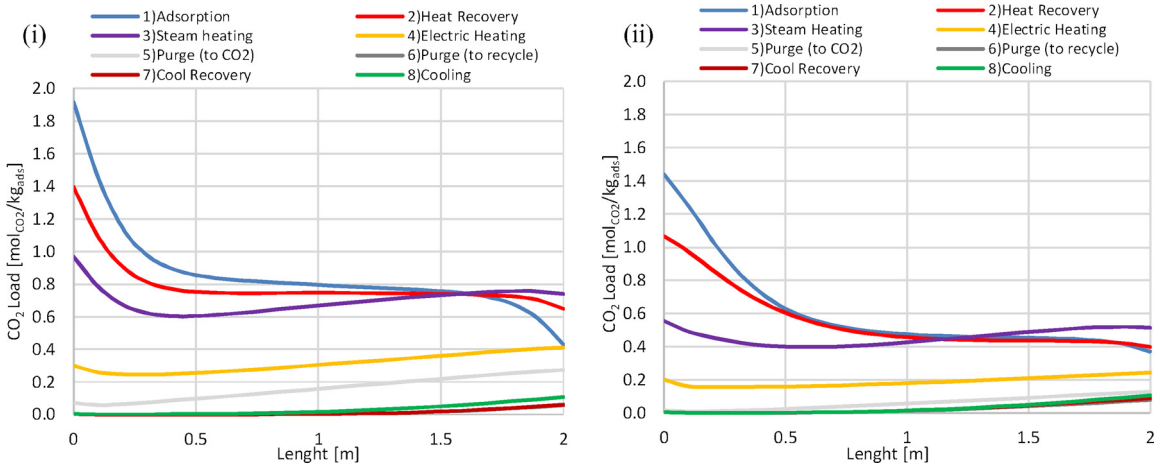

Fig. 13. (i) the CO_2 loading profile at the end of each stage of the process presented in the Appendix A, and (ii) the CO_2 loading profile at the end of each stage of the process for the NGCC case.

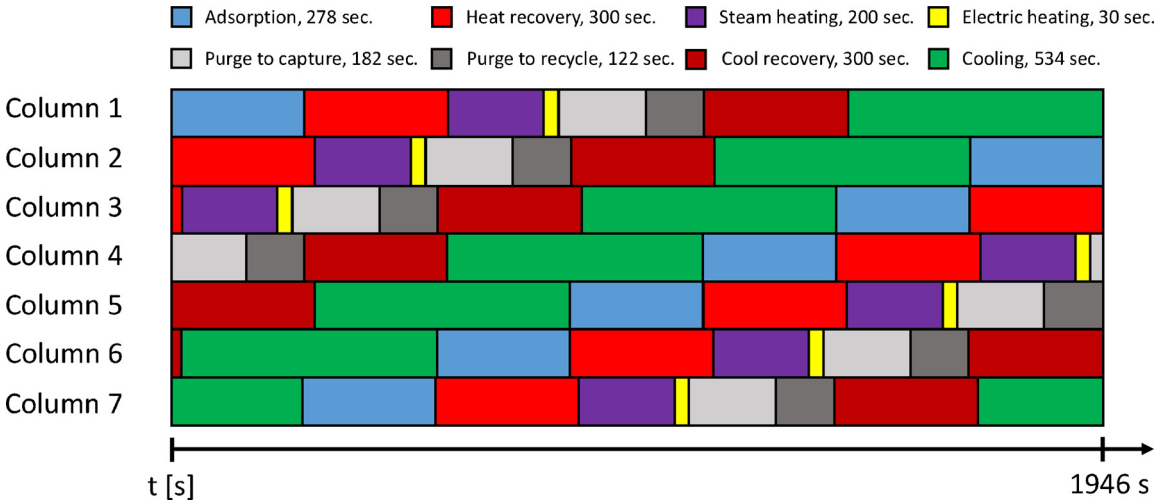

Fig. 14. Scheduling of the T/ESA cycle applied to the NGCC with EGR power plant.

chart is higher than the CO_2 solid load of the second chart because the CO_2 concentration in the flue gas is higher (12% vs 7.26%) so a higher partial pressure increases the saturation of the adsorption bed. On the other hand, the same CO_2 concentration at the end of the desorption step means a higher cyclic capacity and productivity of the material.

The result of the T/ESA material productivity is 49.68 [$kg_{CO2}/(t\ h)$]. This value depends on the cycle time and the CO_2 captured in each cycle. The increment of the CO_2 concentration in the flue gas has the effect to reduce the adsorption time (and consequently the cycle time) and also to rise the loading of the adsorption bed together with CO_2 captured in each cycle. These two effects increase the productivity of the adsorption material with respect to the NGCC case without EGR. Table 5 reports the performance of the T/ESA cycle (the meaning of each parameter is defined in paragraph 3.3).

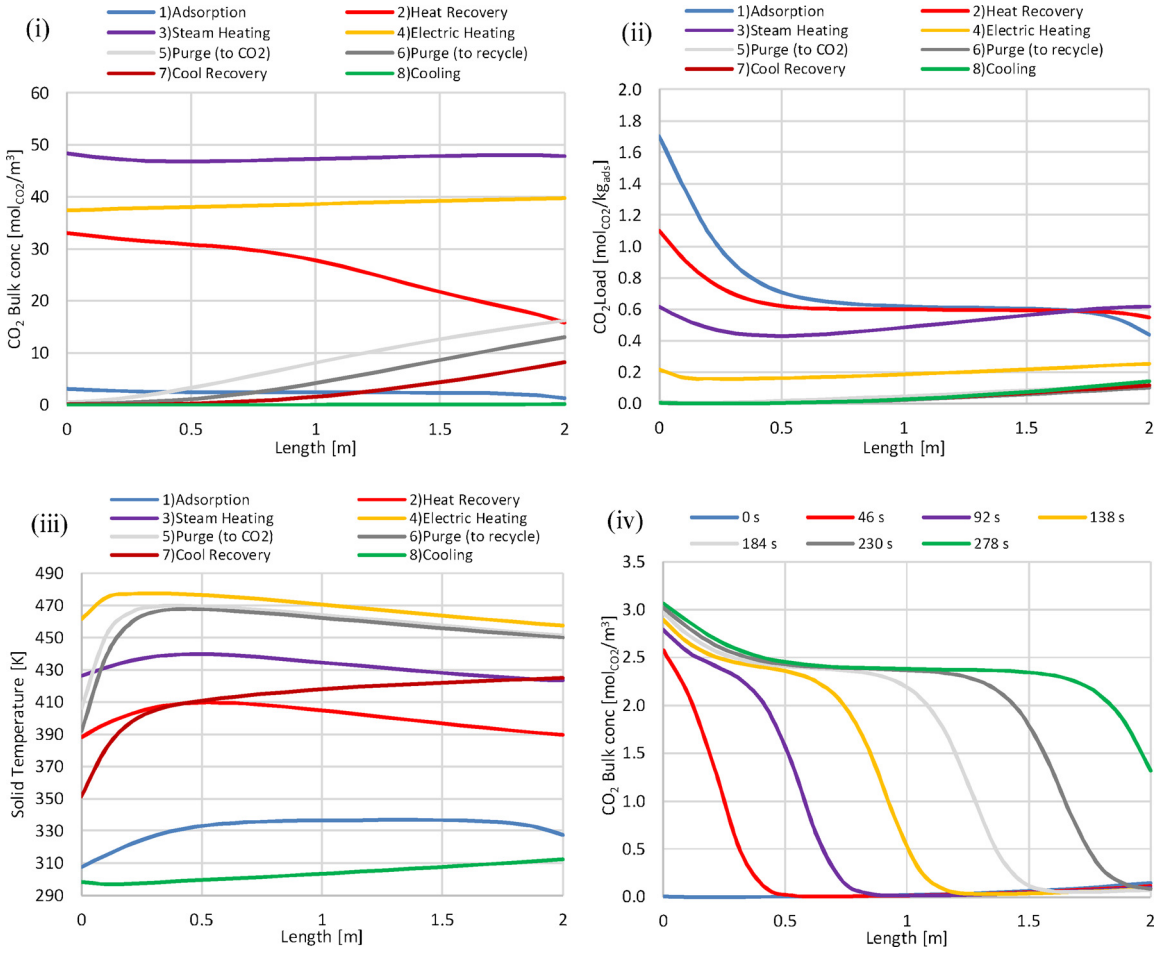

Fig. 15. The four charts present the results for the case with the NGCC + EGR flue gas of: (i) the bulk concentration profile of the CO_2 at the end of each step of the process, (ii) the CO_2 load profile at the end of each step of the process, (iii) the solid temperature profile at the end of each step of the process and (iv) the CO_2 bulk concentration in the column during the adsorption phase at different times.

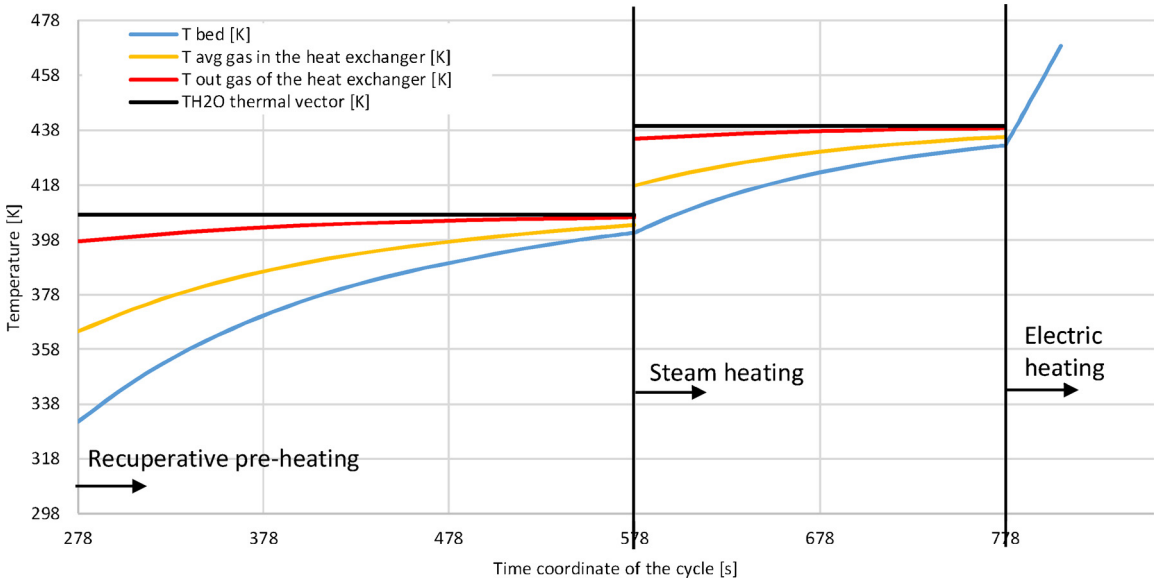

Fig. 16. Average temperature of the column during the heating steps of the T/ESA cycle applied to capture CO_2 from a NGCC + EGR power plant.

The specific consumptions with respect to the case of NGCC without EGR reduces thanks to the higher CO_2 concentration in the exhaust.

5.3. Comparison of T/ESA and MEA technology applied to NGCC power plant

This section summarizes the overall consumptions required to capture the CO_2. Compared to the results above presented, the CO_2 compression work is included together with fan consumption upstream the T/ESA process, and the losses due to the integration with the power plant with the assumptions described in paragraph 3.3.

The overall performance of the considered cases, together with the MEA reference case and the NGCC without CO_2 capture are reported in Table 6. Significant penalties with respect to the MEA reference case can be noted. These are related to the electricity consumption for sorbent regeneration (up to 160 MW) as well fan consumptions (up to 90 MW). The consumption for the sorbent regeneration depends on the process and material considered. The consumption for the fan depends on the configuration of the heat exchangers. The configuration used in this study here presented requires a large amount of flue gas in the PCHE to maintain a convenient heat transient times and avoid the idle times in the scheduling of the process. Starting from a 58.3% of the net electric efficiency of the NGCC plant without CO_2 capture, the overall net electric efficiency for the T/ESA process is 35.3% without EGR and 38.9% with EGR against the 49.9% of the MEA one.

The index used to evaluate the impact of carbon capture in the power plant is the SPECCA (Specific Primary Energy Consumption for Carbon avoided) which is defined in equation (13). SPECCA in T/ESA cases are three or four times higher than in the MEA case (13.05 MJ_{LHV}/kg_{CO2} and 9.64 MJ_{LHV}/kg_{CO2} against 3.36 MJ_{LHV}/kg_{CO2}) despite the heat supplied for the CO_2 regeneration (which is the specific heat duty for the sorbent regeneration minus the heat recovered) are quite close between the two technologies (around 3 and 4 MJ/kg_{CO2}). The reason is that in T/ESA process the heat is supplied by electricity and the fan electric consumption for the heating and cooling process is very high, so it rises a lot the primary energy consumption with respect to the steam

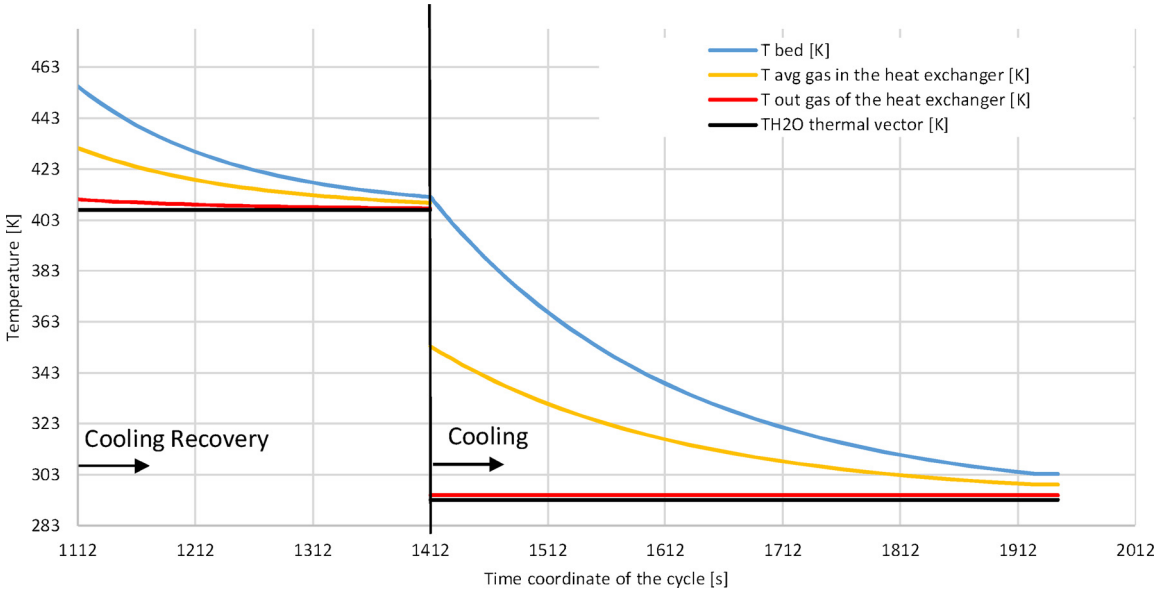

Fig. 17. Average temperature of the column during the cooling transient of the T/ESA cycle applied to capture CO_2 from a NGCC + EGR power plant.

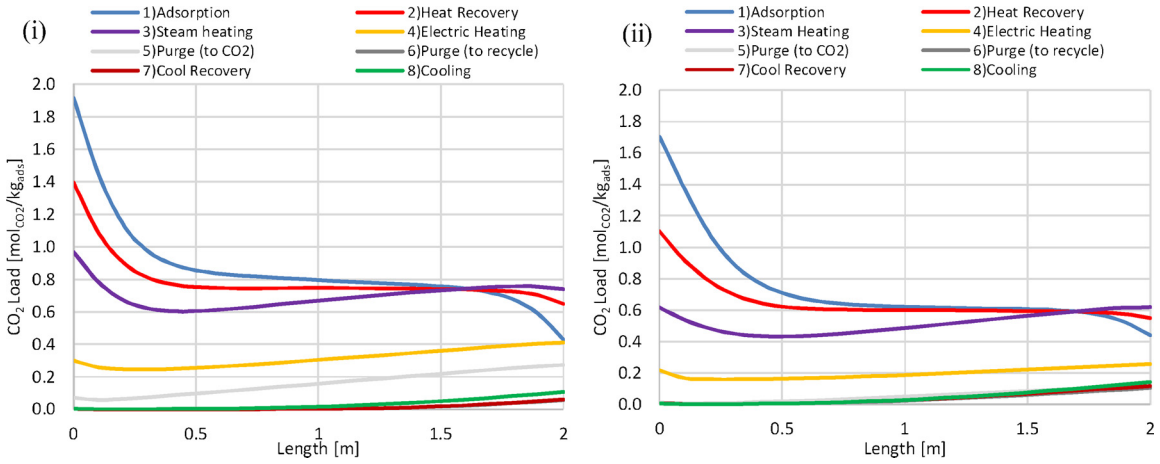

Fig. 18. (i) the CO_2 loading profile at the end of each stage of the process presented in the Appendix A, and (ii) the CO_2 loading profile at the end of each stage of the process for the NGCC + EGR case here presented.

Table 5
Performance of T/ESA process applied to NGCC with EGR power plant.

Parameter	Value
Molar flow of flue gas treated by each column train [kmol/s]	0.75
Carbon capture ratio (CCR) [%]	93.60
CO_2 purity [%]	95.06
Specific heat recovered (HD_{rec}) [MJ/$kg_{CO2capt}$]	2.457
Specific heat duty by steam bleeding (HD_{steam}) [MJ/$kg_{CO2capt}$]	1.073
Specific fan power recovered as heat duty ($w_{fans,rec}$) [MJ/$kg_{CO2capt}$]	0.45
Specific heat duty by electricity (HD_{el}) [MJ/$kg_{CO2capt}$]	1.662
Specific heat Duty ($HD = HD_{rec} + HD_{steam} + w_{fans,rec} + HD_{el}$) [MJ/$kg_{CO2capt}$]	5.642
Specific fan electric duty ($w_{el,fans}$) [MJ/$kg_{CO2capt}$]	1.02
Specific electric penalty due to the steam bleeding ($w_{el,lossST}$) [MJ/$kg_{CO2capt}$]	0.335
Total specific electric penalty ($HD_{el} + w_{el,fans} + w_{el,lossST}$) [MJ/$kg_{CO2capt}$]	3.017

bleeding at 4 bar from the steam turbine required in the MEA plant where for each MJ_{th} of latent heat the electric loss is around 0.25 MJ_{el}.

Comparing the two T/ESA cases with and without the EGR, the latter reduces the value of SPECCA from 13.05 MJ_{LHV}/kg_{CO2} to 9.64 MJ_{LHV}/kg_{CO2}. Indeed, EGR increases the CO_2 concentration in the flue gases and it increases the CO_2 captured in every T/ESA cycle. Since the highest share of the heating energy is provided for the sorbent heating, the amount of energy remains almost constant for every cycle reducing the SPECCA. Another benefit of the EGR on NGCC with this kind of application is the reduction of the exhaust mass flow. Consequently, the volumetric flow treated by the T/ESA plant is lower, and the number of the column needed to treat exhaust gases with a reduction of the investment costs. This fact is identified by an higher productivity of the adsorbent material (49.68 $kg_{CO2}/(t\ h)$ with EGR against 34.57 $kg_{CO2}/(t\ h)$). Finally, the higher CO_2 concentration with the EGR allows higher purities and CCR reducing the CO_2 specific emissions.

Table 6
Results of the integration between NGCC plant and MEA absorption carbon capture plant (i), NGCC and T/ESA carbon capture plant and NGCC with EGR and T/ESA carbon capture plant.

	NGCC	NGCC + EGR	NGCC + MEA	NGCC + T/ESA	NGCC + EGR + T/ESA
Exhaust mass flow [kg/s]	1330.6	831.7	1259.9	1257.4	751.0
CO_2 emitted [kg/s]	80.3	86.2	9.6	7.1	5.5
CO_2 captured [kg/s]	–	–	70.7	73.2	80.7
N° of gas turbine	2	2	2	2	2
Gas Turbine [MW]	272.1	285.0	272.1	272.1	285.0
Steam Cycle Gross Power, [MW]	292.4	321.0	215.7	263.4	294.0
Steam Cycle auxiliaries, [MW]	−3.4	−3.4	−3.4	−3.4	−3.4
CO_2 compressor, [MW]	–	–	−22.6	−27.2	−29.8
Exhaust gas fans, [MW]	–	–	−15	−15	−15
Fan EGR	–	−6.9	–	–	−6.9
Aux. for heat rejection, [MW]	−3.7	−3.7	−4.4	−4.1	−4.1
T/ESA fan consumptions [MW]	–	–	–	−89.2	−82.4
Chiller consumptions [MW]	–	–	–	−3.6	−3.6
Electric consumption for sorbent regeneration [MW]	–	–	–	−156.0	−134.2
Other auxiliaries [MW]	–	–	−4.6	–	–
Net Power Output, [MW]	829.5	877.0	709.9	509.1	584.3
Thermal Power $Input_{LHV}$, [MW]	1422.6	1503.0	1422.6	1422.6	1503.0
Net Electric Efficiency (on LHV), [%]	58.3	58.3	49.90	35.3	38.9
Emissions [kg_{CO2}/MWh_{el}]	351.8	351.8	42.36	49.9	34.0
CO_2 avoided, [%]	–	–	88.0	91.2	93.6
CO_2 purity, [%]	–	–	100.0	94.7	95.1
SPECCA (MJ_{LHV}/kg_{CO2})	–	–	3.36	13.05	9.64
N° Column trains	–	–	–	74	40
N° Column per trains				5	7
N° Columns total	–	–	–	370	280

6. Conclusions

The thermodynamic assessment of the Temperature Electric Swing Adsorption (T/ESA) process integrated to NGCC power plants is studied. The T/ESA process is modelled using Aspen Adsorption and integrated with a heat transient model to account for the heating/cooling steps of the process for the sorbent regeneration. A water removal section upstream the T/ESA process is considered to limit the competitive water/CO_2 adsorption in the zeolite material used for CO_2 capture. The T/ESA process is applied to two different cases: a standard NGCC power plant and an NGGC with EGR power plant. Then the overall performance of these two cases are compared with a benchmark NGCC integrated with a MEA carbon capture plant.

The overall net electric efficiency of the NGCC with T/ESA technology is 35.3% while with EGR is 38.9%. Indeed, EGR does not penalize the efficiency of the NGCC power plant but it increases the CO_2 concentration in the exhaust gas treated by the capture plant. It increases the efficiency of the T/ESA plant in terms of SPECCA (9.64 MJ_{LHV}/kg_{CO2} against 13.305 MJ_{LHV}/kg_{CO2}), CCR (93.6% against 91.2%) and CO_2 specific emissions (34.0 kg_{CO2}/MWh_{el} against 50 kg_{CO2}/MWh_{el}). Moreover, EGR reduces the exhaust gas mass flow reducing the amount of column in the T/ESA plant (280 against 370) increasing the productivity of the adsorbent material (49.68 $kg_{CO2}/(t\ h)$ with EGR against 34.57 $kg_{CO2}/(t\ h)$) with a reduction of the investment costs.

Compared to T/ESA process, the net electric efficiency of a NGCC with the MEA absorption plant is significantly higher and equal to 49.9%. The same results are confirmed by the SPECCA index 13.05 MJ_{LHV}/kg_{CO2} to 9.64 MJ_{LHV}/kg_{CO2} against 3.36 MJ_{LHV}/kg_{CO2}.

With respect to the MEA, the energy penalty of the T/ESA is significant because of electric regeneration and fan consumptions during the heating/cooling steps of the sorbent regeneration. The energetic value of electric power is about 5 times higher than low temperature heat used in competitive technologies (i.e. amine scrubbing). Indeed, the regeneration temperature of the MEA is around 120 °C, so the steam extracted for the column heating comes from the low pressure section of the steam turbine which has a report between electric loss on heat extracted around 0.2-0.25. These results are the first attempt to simulate a T/ESA process using different heat sources for sorbent regeneration. With the selected material and the plant configuration designed, the analysis shows that T/ESA is uncompetitive when applied to NGCC's. New material development may improve the performance of the process. In addition, further investigation on the cycling of the T/ESA unit, aiming to reduce pressure drop costs and capital expenditure, must be performed.

Acknowledgements

The research leading to these results has received funding from the European Union Seventh Framework Programme (FP7 2007–2013) under Grant Agreement 608534 (MATESA project). Web-page: www.sintef.com/matesa.

Appendix A. T/ESA model validation with existing literature

The T/ESA process described in detail in the previous Section 2 was applied to exhaust gases reported in a previous publication available in literature (Joss et al., 2017). This preliminary analysis was performed to validate the developed methodology and the consequent results.

This validation aims to check the assumptions of the model and their implementation in the Aspen model. The validation case by Joss et al. presents the results for a TSA with a very similar adsorption cycle and a standard shaped Zeolite 13X (with slightly different properties with respect to the honeycomb used in T/ESA process). Moreover, the performance optimization of the process is the result of the Pareto curve identified by thousands of cases run with different time scheduling. In the present work a Pareto analysis for the optimization of the process was not performed, so the validation test gives a feedback on both the modeling of the adsorption process, and how the performance here presented are close to the Pareto curve.

The channel dimensions and the column length were selected to maximize adsorption properties, while limiting the pressure drop. These properties are listed in Table A1. Indeed, during the heating steps, the fans blow a large mass flow of gas for long time, hence the fan power consumption is one of the main electric consumptions of the capture plant.

Table A1
Geometric parameters of the adsorption bed and honeycomb adsorbent.

Parameter	Value
Column height [m]	2
Column diameter [m]	6
Bed void fraction [−]	0.657
Channel side length [m]	0.0047
Wall thickness [m]	0.0011

The geometric parameters of the column remained constant in every case considered in this paper.

Case with 12% of molar CO_2 concentration and overall performances of the cycle

The first case considered assumes a CO_2 concentration of 12% at capture process inlet (N_2 equal to 88%), featuring a typical exhaust gas composition of coal plants.

A preliminary analysis was performed to investigate the characteristic time of each cycle step to optimize the time scheduling of the process. However, the number of cases performed are not enough to draw a Pareto curve, therefore it cannot be stated that the final results are the optimal ones. To assess the quality of the process optimization, results are compared with the ones determined with a real TSA optimization process presented by (Joss et al., 2017). The performance of the T/ESA cycle is reported in Table A2 (the meaning of each parameter is defined in paragraph 3.2).

The performance of the simulation of T/ESA in Aspen is in agreement with the optimized ones presented by (Joss et al., 2017). Indeed, the results of the optimized TSA cycle proposed by (Joss et al., 2017) has a CCR of 97.1%, a CO_2 purity of 98.2% and a specific heat duty of 4.39 $MJ/kg_{CO2capt}$. Considering that there are some discrepancies on the assumptions and the adsorption cycle steps, the values found with the Aspen model can be considered reliable and representative of close-to-optimized case.

Table A2
Performance of T/ESA process with 12% of CO_2 concentration.

Parameter	Value
Molar flow of flue gas treated by each column train [kmol/s]	0.69
Carbon capture ratio (CCR) [%]	97.10
CO_2 purity [%]	96.90
Specific heat recovered (HD_{rec}) [MJ/$kg_{CO2capt}$]	1.68
Specific heat duty by steam bleeding (HD_{steam}) [MJ/$kg_{CO2capt}$]	0.84
Specific fan power recovered as heat duty ($w_{fans,rec}$) [MJ/$kg_{CO2capt}$]	0.46
Specific heat duty by electricity (HD_{el}) [MJ/$kg_{CO2capt}$]	1.59
Specific heat Duty ($HD = HD_{rec} + HD_{steam} + w_{fans,rec} + HD_{el}$) [MJ/$kg_{CO2capt}$]	4.57
Specific fan electric duty ($w_{el,fans}$) [MJ/$kg_{CO2capt}$]	1.04
Specific electric penalty due to the steam bleeding ($w_{el,lossST}$) [MJ/$kg_{CO2capt}$]	0.23
Total specific electric penalty ($HD_{el} + w_{el,fans} + w_{el,lossST}$) [MJ/$kg_{CO2capt}$]	2.86

The cycle scheduling is designed with the simplified graphical approach explained by (Mehrotra et al., 2011) considering the constrain due to the time matching between a recuperative pre-heating phase and a thermal recovery phase. The heating and cooling times, consequently fan power, are determined to avoid idle time and limit the pressure losses by reducing the gas velocity in the bed. The scheduling is reported in Fig. A1.

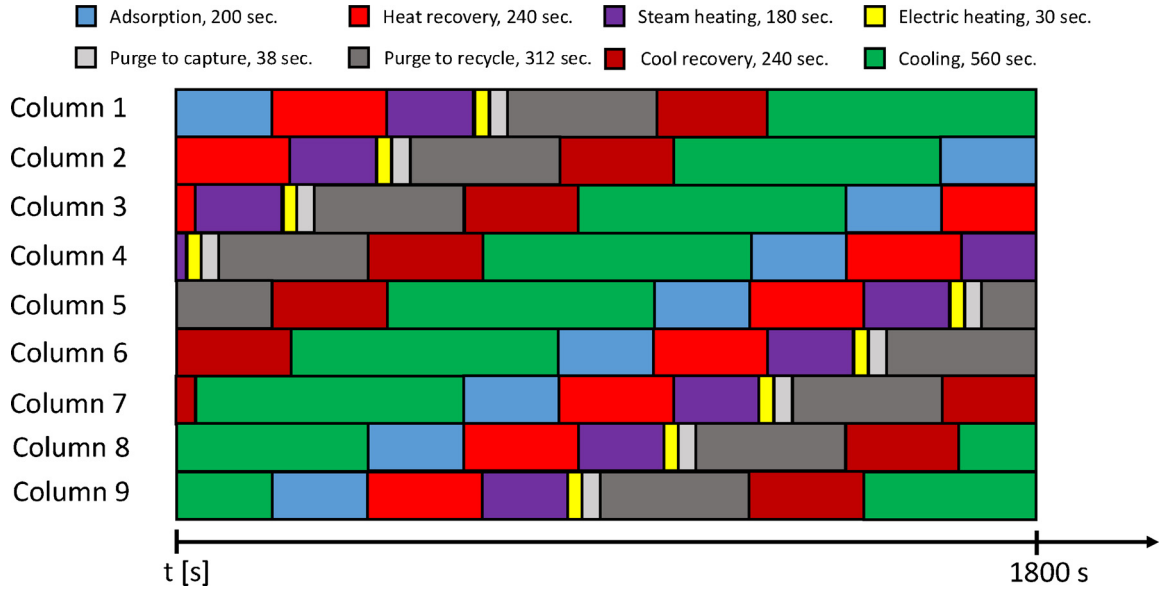

Fig. A1. Scheduling of the T/ESA cycle with flow 12% CO_2 concentration in the flue gases.

The result is a train composed by 9 columns with a diameter of 6 m and a height of 2 m and a cycle of 1800seconds. Other interesting results are the bed profiles of the temperature and sorbent CO_2 loading at the end of each step (see Fig. A2). In addition, the CO_2 bulk concentration at the end of each step as well during the adsorption step. The first chart in Fig. A2 describes the desorption process step by step where the bulk concentration in the gas phase inside the column rises together with the temperature during the heating step desorbing the CO_2. The second chart in Fig. A2 shows the solid loading. Since at the end of the adsorption step the solid is almost at the equilibrium with the CO_2 adsorption (except for the outlet part), it can be noted the impact of the temperature profile of the column (presented in the third chart in Fig. A2) on the CO_2 load of the solid: the temperature at the end of the adsorption step is lower at the beginning of the column (325 K) than in the central part where it is almost constant around 350 K. According to the temperature profile, the solid CO_2 loading is higher at the inlet of the column (almost the double) than in the central part. Indeed, observing the isotherms of the material in Fig. 3, the effect of the temperature on the material loading is very high at low partial pressures. The forth chart in Fig. A2 shows the CO_2 concentration in the gas phase in the column during the adsorption step. The adsorption step stops when CO_2 stats leaving the column because of the saturation of the solid, indeed at 200 s the CO_2 concentration at the outlet is not close to zero like at the other times.

The heating and cooling transient steps are reported in Figs. A3 and Fig. A4. In Fig. A3, the three different heating steps are outlined: recuperative pre-heating, steam and the electric heating. The recuperative pre-heating and the steam heating part are similar for what concerns the heat transfer and the difference of temperature between the vector fluid and the bed, while the electric heating is faster and represented by a strict line.

Fig. A4 shows two different parts, the cooling recovery and the cooling steps. The cooling recovery step is coupled with the heating recovery step previously discussed, indeed also the duration of the step coincides. The difference of temperature between the beginning and the end of the

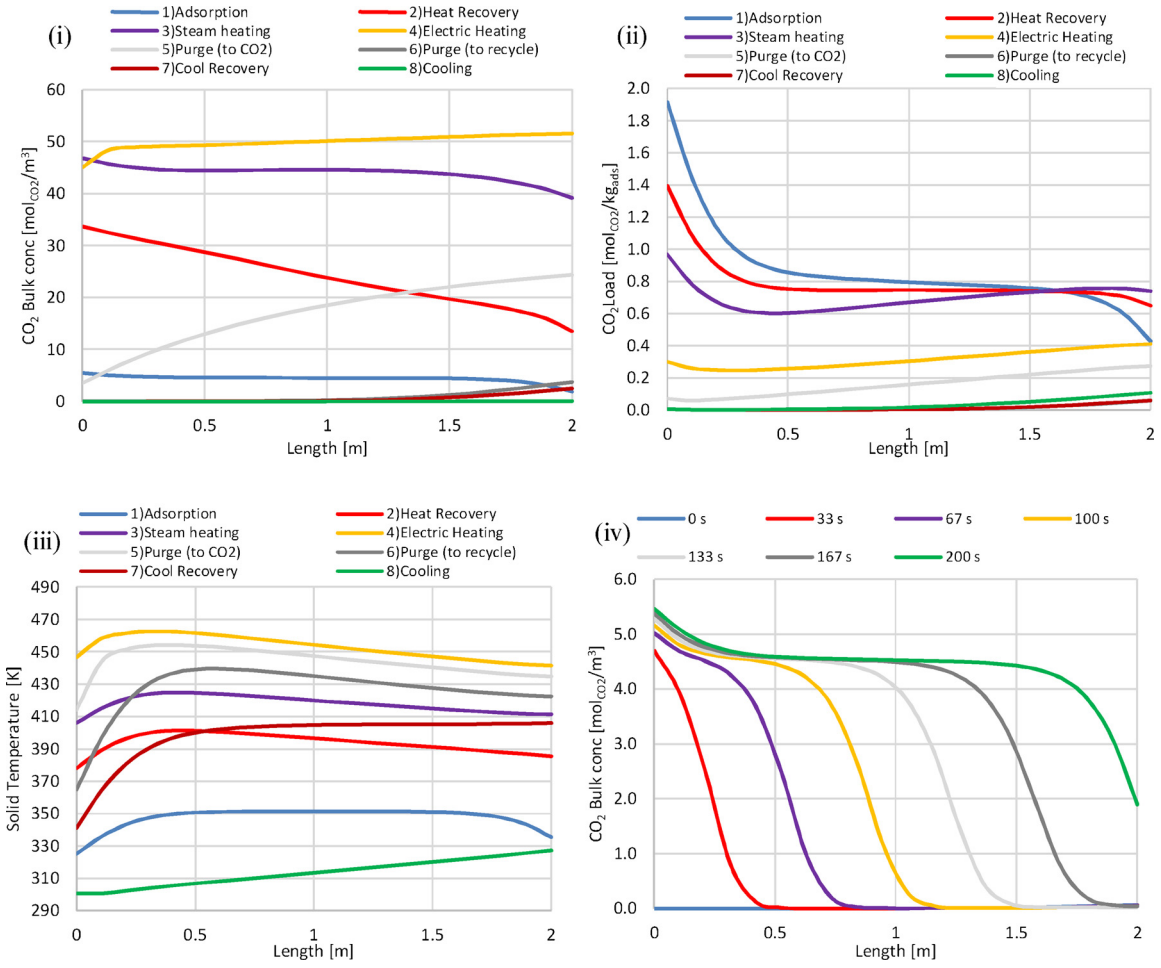

Fig. A2. The four charts present the results for the validation case of: (i) the bulk concentration profile of the CO_2 at the end of each stage of the process, (ii) the CO_2 load profile at the end of each stage of the process, (iii) the solid temperature profile at the end of each stage of the process and (iv) the CO_2 bulk concentration in the column during the adsorption phase at different time frames.

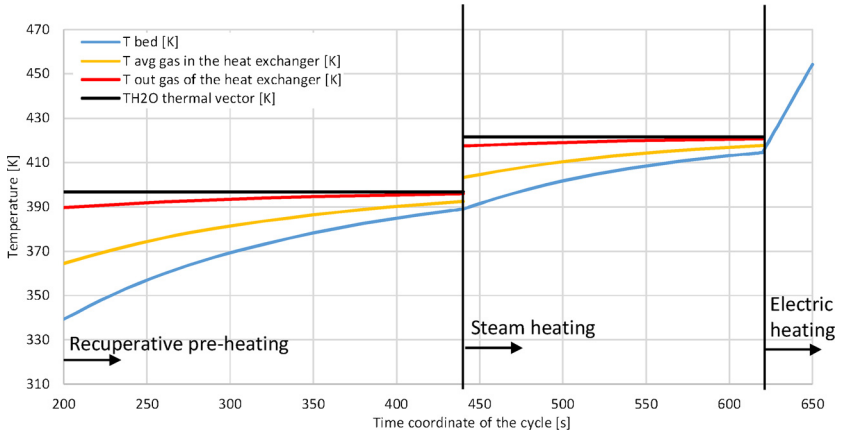

Fig. A3. Average temperature of the column on the time coordinate of the cycle during the heating step of the T/ESA cycle with flow 12% CO_2 concentration in the flue gases.

recuperative pre-heating step is higher than the difference of temperature between the beginning and the end of the cooling recovery step. This is due to the fans power needed for the gas circulation in the column that increase the difference of temperature in the heating step and reduce it in the cooling step. The cooling step, where the bed is cooled with cooling water, is the longest step.

Finally, knowing the amount of CO_2 captured in each cycle and the adsorbent material involved in each column train, the productivity of the material ΠIads, as defined in Eq. (5), is 56.63 [kg_{CO2}/(t h)] (as term of comparison, (Joss et al., 2017) report values between 35 [kg_{CO2}/(t h)] and 50 [kg_{CO2}/(t h)] for cases with CCR greater than 90% and a purity of CO_2 (ϕ) greater than 96%).

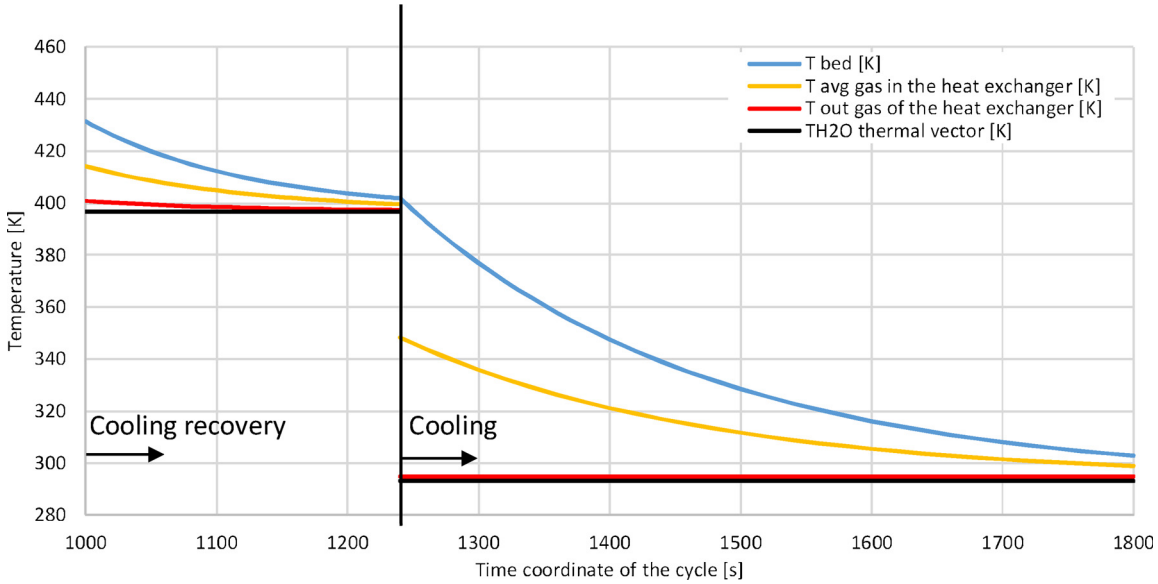

Fig. A4. Average temperature of the column on the time coordinate of the cycle during the cooling step of the T/ESA cycle with flow 12% CO_2 concentration in the flue gases.

References

Aspentech, 2003. Aspen Adsim™ 12.1.

Banks, B., Bibland-Pritchard, M., 2015. SaskPower's Carbon Capture Project | Canadian Centre for Policy Alternatives 24.

Bonalumi, D., Giuffrida, A., 2016. Investigations of an air-blown integrated gasification combined cycle fired with high-sulphur coal with post-combustion carbon capture by aqueous ammonia. Energy. http://dx.doi.org/10.1016/j.energy.2016.04.025.

Bonalumi, D., Valenti, G., Lillia, S., Fosbøl, P.L., Thomsen, K., 2016. A layout for the carbon capture with aqueous ammonia without salt precipitation. Energy Procedia 86, 134–143. http://dx.doi.org/10.1016/j.egypro.2016.01.014.

Bonnissel, M.P., Luo, L., Tondeur, D., 2001. Rapid thermal swing adsorption. Ind. Eng. Chem. Res. 40, 2322–2334. http://dx.doi.org/10.1021/ie000809k.

Burchell, T.D., Judkins, R.R., Rogers, M.R., Williams, A.M., 1997. A novel process and material for the separation of carbon dioxide and hydrogen sulfide gas mixtures. Carbon N. Y. 35, 1279–1294. http://dx.doi.org/10.1016/S0008-6223(97)00077-8.

Cavenati, S., Grande, C.A., Rodrigues, A.E., 2004. Adsorption equilibrium of methane, carbon dioxide, and nitrogen on zeolite 13X at high pressures. J. Chem. Eng. Data 49, 1095–1101. http://dx.doi.org/10.1021/je0498917.

Dostal, V., 2004. A Supercritical Carbon Dioxide Cycle. Massachusetts Institute of Technology.

Evulet, A.T., El Kady, A.M., Branda, A.R., Chinn, D., 2009. On the performance and operability of GE's dry low NOx combustors utilizing exhaust gas recirculation for postcombustion carbon capture. Energy Procedia 1, 3809–3816. http://dx.doi.org/10.1016/j.egypro.2009.02.182.

Gazzani, M., Turi, D.M., Ghoniem, A.F., Macchi, E., Manzolini, G., 2014. Techno-economic assessment of two novel feeding systems for a dry-feed gasifier in an IGCC plant with Pd-membranes for CO2 capture. Int. J. Greenh. Gas Control 25, 62–78. http://dx.doi.org/10.1016/j.ijggc.2014.03.011.

Girimonte, R., Formisani, B., Testa, F., 2017. Adsorption of CO 2 on a confined fluidized bed of pelletized 13X zeolite. Powder Technol. 311, 9–17. http://dx.doi.org/10.1016/j.powtec.2017.01.033.

Giuffrida, A., Bonalumi, D., Lozza, G., 2013. Amine-based post-combustion CO2 capture in air-blown IGCC systems with cold and hot gas clean-up. Appl. Energy 110, 44–54. http://dx.doi.org/10.1016/j.apenergy.2013.04.032.

Gkanas, E.I., Steriotis, T.A., Stubos, A.K., Myler, P., Makridis, S.S., 2015. A complete transport validated model on a zeolite membrane for carbon dioxide permeance and capture. Appl. Therm. Eng. 74, 36–46. http://dx.doi.org/10.1016/j.applthermaleng.2014.02.006.

Grande, C.A., Rodrigues, A.E., 2008. Electric Swing Adsorption for CO2 removal from flue gases. Int. J. Greenh. Gas Control 2, 194–202. http://dx.doi.org/10.1016/S1750-5836(07)00116-8.

Grande, C.A., Ribeiro, R.P.L., Oliveira, E.L.G., Rodrigues, A.E., 2009. Electric swing adsorption as emerging CO2 capture technique. Energy Procedia 1, 1219–1225. http://dx.doi.org/10.1016/j.egypro.2009.01.160.

Jansen, D., Gazzani, M., Manzolini, G., Van Dijk, E., Carbo, M., 2015. Pre-combustion CO2 capture. Int. J. Greenh. Gas Control 40, 167–187. http://dx.doi.org/10.1016/j.ijggc.2015.05.028.

Joss, L., Gazzani, M., Mazzotti, M., 2017. Rational design of temperature swing adsorption cycles for post-combustion CO2 capture. Chem. Eng. Sci. 158, 381–394. http://dx.doi.org/10.1016/j.ces.2016.10.013.

Kenarsari, S.D., Yang, D., Jiang, G., Zhang, S., Wang, J., Russell, A.G., Wei, Q., Fan, M., 2013. Review of recent advances in carbon dioxide separation and capture. RSC Adv. 3, 22739. http://dx.doi.org/10.1039/c3ra43965h.

Kim, H., Lee, K.S., 2017. Energy analysis of an absorption-based CO2capture process. Int. J. Greenh. Gas Control 56, 250–260. http://dx.doi.org/10.1016/j.ijggc.2016.12.002.

Kvamsdal, H.M., Romano, M.C., van der Ham, L., Bonalumi, D., van Os, P., Goetheer, E., 2014. Energetic evaluation of a power plant integrated with apiperazine-based CO2capture process. Int. J. Greenh. Gas Control 28, 343–355.

Li, H., Ditaranto, M., Berstad, D., 2011. Technologies for increasing CO2 concentration in exhaust gas from natural gas-fired power production with post-combustion, amine-based CO2 capture. Energy 36, 1124–1133. http://dx.doi.org/10.1016/j.energy.2010.11.037.

Li, T., Dietiker, J.-F., Rogers, W., Panday, R., Gopalan, B., Breault, G., 2016. Investigation of CO2 capture using solid sorbents in a fluidized bed reactor: cold flow hydrodynamics. Powder Technol. 301, 1130–1143. http://dx.doi.org/10.1016/j.powtec.2016.07.056.

Lindqvist, K., Jordal, K., Haugen, G., Hoff, K.A., Anantharaman, R., 2014. Integration aspects of reactive absorption for post-combustion CO2 capture from NGCC (natural gas combined cycle) power plants. Energy 78, 758–767. http://dx.doi.org/10.1016/j.energy.2014.10.070.

Mérel, J., Clausse, M., Meunier, F., 2006. Carbon dioxide capture by indirect thermal swing adsorption using 13X zeolite. Environ. Prog. 25, 327–333. http://dx.doi.org/10.1002/ep.10166.

Masala, A., Vitillo, J.G., Bonino, F., Manzoli, M., Grande, C.A., Bordiga, S., 2016. New insights into UTSA-16. Phys. Chem. Chem. Phys. 18, 220–227. http://dx.doi.org/10.1039/C5CP05905D.

Masala, A., Vitillo, J.G., Mondino, G., Martra, G., Blom, R., Grande, C.A., Bordiga, S., 2017. Conductive ZSM-5-based adsorbent for CO2 capture: active phase vs monolith. Ind. Eng. Chem. Res. 56, 8485–8498. http://dx.doi.org/10.1021/acs.iecr.7b01058.

Mehrotra, A., Ebner, A.D., Ritter, J.A., 2011. Simplified graphical approach for complex PSA cycle scheduling. Adsorption 17, 337–345. http://dx.doi.org/10.1007/s10450-011-9326-6.

Petkovska, M., Tondeur, D., Grevillot, G., Granger, J., Mitrović, M., 1991. Temperature-swing gas separation with electrothermal desorption step. Sep. Sci. Technol. 26, 425–444. http://dx.doi.org/10.1080/01496399108050482.

Ribeiro, R.P.P.L., Grande, C.A., Rodrigues, A.E., 2012. Electrothermal performance of an activated carbon honeycomb monolith. Chem. Eng. Res. Des. 90, 2013–2022. http://dx.doi.org/10.1016/j.cherd.2012.03.010.

Ribeiro, R.P.P.L., Grande, C.A., Rodrigues, A.E., 2013. Activated carbon honeycomb monolith – zeolite 13X hybrid system to capture CO2 from flue gases employing electric swing adsorption. Chem. Eng. Sci. 104, 304–318. http://dx.doi.org/10.1016/j.ces.2013.09.011.

Ribeiro, R.P.P.L., Grande, C.A., Rodrigues, A.E., 2014. Electric swing adsorption separation and purification: a review. Sep. Sci. Technol. 49, 1985–2002. http://dx.doi.org/10.1080/01496395.2014.915854.

Sanchez Fernandez, E., Goetheer, E.L.V., Manzolini, G., Macchi, E., Rezvani, S., Rezvani, T.J.H., 2014. Thermodynamic assessment of amine based CO2 capture technologies in power plants based on European benchmarking task force methodology. Fuel 129, 318–329. http://dx.doi.org/10.1016/j.fuel.2014.03.042.

Sipöcz, N., Tobiesen, F.A., 2012. Natural gas combined cycle power plants with CO2 capture – opportunities to reduce cost. Int. J. Greenh. Gas Control 7, 98–106. http://dx.doi.org/10.1016/j.ijggc.2012.01.003.

Song, C., Kansha, Y., Ishizuka, M., Fu, Q., Tsutsumi, A., 2015. Chemical engineering and processing: process intensi fi cation conceptual design of a novel pressure swing CO 2

adsorption process based on self-heat recuperation technology. Chem. Eng. Process. Process Intensif. 94, 20–28. http://dx.doi.org/10.1016/j.cep.2015.03.008.
Subrenat, A.S., Le Cloirec, P.A., 2006. Volatile organic compound (Voc) removal by adsorption onto activated carbon fiber cloth and electrothermal desorption: an industrial application. Chem. Eng. Commun. 193, 478–486. http://dx.doi.org/10.1080/00986440500191768.
Sullivan, P.D., Rood, M.J., Grevillot, G., Wander, J.D., Hay, K.J., 2004. Activated carbon fiber cloth electrothermal swing adsorption system. Environ. Sci. Technol. 38, 4865–4877. http://dx.doi.org/10.1021/es0306415.
Thakur, R.S., Kaistha, N., Rao, D.P., 2015. Chemical engineering and Processing: process Intensi fi cation Novel single-bed and twin-bed pressure swing adsorption systems. Chem. Eng. Process. Process Intensif. 95, 165–174. http://dx.doi.org/10.1016/j.cep.2015.06.003.
Van der Spek, M., Bonalumi, D., Manzolini, G., Ramirez, A., Faaij, A., 2018. Techno-economic comparison of combined cycle gas turbines with advanced membrane configuration and MEA solvent at part load conditions. Energy Fuels 32, 625–645.
Vitillo, J.G., Smit, B., Gagliardi, L., 2017. Introduction: carbon capture and separation. Chem. Rev. 117, 9521–9523. http://dx.doi.org/10.1021/acs.chemrev.7b00403.
Wang, M., Lawal, A., Stephenson, P., Sidders, J., Ramshaw, C., 2011. Post-combustion CO2 capture with chemical absorption: a state-of-the-art review. Chem. Eng. Res. Des. 89, 1609–1624. http://dx.doi.org/10.1016/j.cherd.2010.11.005.
Xiang, S., He, Y., Zhang, Z., Wu, H., Zhou, W., Krishna, R., Chen, B., 2012. Microporous metal-organic framework with potential for carbon dioxide capture at ambient conditions. Nat. Commun. 3, 954–959. http://dx.doi.org/10.1038/ncomms1956.
Yaumi, A.L., Bakar, M.Z.A., Hameed, B.H., 2017. Recent advances in functionalized composite solid materials for carbon dioxide capture. Energy 124, 461–480. http://dx.doi.org/10.1016/j.energy.2017.02.053.
Yu, F.D., Luo, L., Grevillot, G., 2007. Electrothermal swing adsorption of toluene on an activated carbon monolith. Chem. Eng. Process. Process Intensif. 46, 70–81. http://dx.doi.org/10.1016/j.cep.2006.04.008.